PHILOSOPHICAL TRANSACTIONS
OF THE ROYAL SOCIETY B
BIOLOGICAL SCIENCES

A new stem-varanid lizard (Reptilia, Squamata) from the early Eocene of China

Journal:	*Philosophical Transactions B*
Manuscript ID	RSTB-2021-0041.R2
Article Type:	Research
Date Submitted by the Author:	21-Oct-2021
Complete List of Authors:	Dong, Li-Ping; Institute of Vertebrate Paleontology and Paleoanthropology Chinese Academy of Sciences; Key Laboratory of Vertebrate Evolution and Human Origins of Chinese Academy of Sciences; CAS Center for Excellence in Life and Paleoenvironment Wang, Yuanqing; Institute of Vertebrate Paleontology and Paleoanthropology Chinese Academy of Sciences; Key Laboratory of Vertebrate Evolution and Human Origins of Chinese Academy of Sciences; CAS Center for Excellence in Life and Paleoenvironment Zhao, Qi; Institute of Vertebrate Paleontology and Paleoanthropology Chinese Academy of Sciences; Key Laboratory of Vertebrate Evolution and Human Origins of Chinese Academy of Sciences; CAS Center for Excellence in Life and Paleoenvironment Vasiliyan, Davit ; JURASSICA Museum, Route de Fontenais 21, 2900 Porrentruy, Switzerland; Department of Geosciences, University of Fribourg, Chemin du musée 6, 1700 Fribourg, Switzerland Wang, Yuan; Key Laboratory of Vertebrate Evolution and Human Origins of Chinese Academy of Sciences; Institute of Vertebrate Paleontology and Paleoanthropology Chinese Academy of Sciences; CAS Center for Excellence in Life and Paleoenvironment Evans, Susan; University College London, Centre for Integrative Anatomy, Department of Cell & Developmental Biology
Issue Code (this should have already been entered and appear below the blue box, but please contact the Editorial Office if it is not present):	FOSSILS
Subject:	Evolution < BIOLOGY, Palaeontology < BIOLOGY
Keywords:	Early Eocene, China, Varanidae, Evolution

Author-supplied statements

Relevant information will appear here if provided.

Ethics

Does your article include research that required ethical approval or permits?:
This article does not present research with ethical considerations

Statement (if applicable):
CUST_IF_YES_ETHICS :No data available.

Data

It is a condition of publication that data, code and materials supporting your paper are made publicly available. Does your paper present new data?:
Yes

Statement (if applicable):
The holotype specimen of Archaeovaranus lii IVPP V 22770 is deposited in the vertebrate collection of the Institute of Vertebrate Paleontology and Paleoanthropology, Chinese Academy of Sciences. The CT models and original data are available on the request of whoever is interested. The data matrix used for the phylogenetic analysis is included and uploaded as supplementary material (Data S1).

Conflict of interest

I/We declare we have no competing interests

Statement (if applicable):
CUST_STATE_CONFLICT :No data available.

Authors' contributions

This paper has multiple authors and our individual contributions were as below

Statement (if applicable):
DLP, WYQ, ZQ, VD, YW, ES wrote and revised the ms. DLP conducted the phylogenetic analysis, made the CT construction, and the illustrations. ZQ made the histological analyses and the related figures.

A new stem-varanid lizard (Reptilia, Squamata) from the early Eocene of China

Liping Dong, Yuan-Qing Wang, Qi Zhao, Davit Vasilyan, Yuan Wang, Susan E. Evans

Liping Dong, Key Laboratory of Vertebrate Evolution and Human Origins, Institute of Vertebrate Paleontology and Paleoanthropology, Chinese Academy of Sciences, Beijing, PR China; CAS Center for Excellence in Life and Paleoenvironment, Beijing, PR China

Yuan-Qing Wang, Key Laboratory of Vertebrate Evolution and Human Origins, Institute of Vertebrate Paleontology and Paleoanthropology, Chinese Academy of Sciences, Beijing, PR China; CAS Center for Excellence in Life and Paleoenvironment, Beijing, PR China

Qi Zhao, Key Laboratory of Vertebrate Evolution and Human Origins, Institute of Vertebrate Paleontology and Paleoanthropology, Chinese Academy of Sciences, Beijing, PR China; CAS Center for Excellence in Life and Paleoenvironment, Beijing, PR China

Davit Vasilyan, JURASSICA Museum, Porrentruy, Switzerland; Department of the Geosciences, University of Fribourg, Fribourg, Switzerland

Yuan Wang, Key Laboratory of Vertebrate Evolution and Human Origins, Institute of Vertebrate Paleontology and Paleoanthropology, Chinese Academy of Sciences, Beijing, PR China; CAS Center for Excellence in Life and Paleoenvironment, Beijing, PR China

Susan E. Evans, Centre for Integrative Anatomy, Department of Cell and Developmental Biology, University College London, London, UK.

Description

This paper describes the well-preserved skull and skeleton of a new genus and species of stem-varanid lizard from the early Eocene of China. Phylogenetic analysis places the new species as the sister taxon of *Varanus*, providing support for an Asian origin for this important lizard genus.

Abstract
Monitor lizards (genus *Varanus*) are today distributed across Asia, Africa and Australasia, and represent one of the most recognizable and successful lizard lineages. They include charismatic living species like the Komodo Dragon of Indonesia and the even larger extinct *Varanus prisca* (*Megalania*) of Australia. The fossil record suggests that living varanids had their origins in a diverse assemblage of stem (varaniform) species known from the Late Cretaceous of China and Mongolia. However, determining the biogeographic origins of crown-varanids has proved problematic, with Asia, Africa, and Australia each being proposed. The problem is complicated by the fragmentary nature of many attributed specimens, and the fact that the most widely accepted, and most complete, fossil of a stem-varanid, that of *Saniwa ensidens*, is from North America. In this paper, we describe a well-preserved skull and skeleton of a new genus of stem-varanid from the Eocene of China. Phylogenetic analysis places the new genus as the sister taxon of *Varanus,* suggesting that the transition from Cretaceous varaniform lizards to *Varanus* occurred in East Asia before the origin and dispersal of *Varanus* to other regions. The discovery of the new specimen thus fills an important gap in the fossil record of monitor lizards. The similar lengths of the fore- and hind limbs in this new taxon are unusual among the total group Varanidae, and suggest it may have had a different lifestyle, at least from the contemporaneous North American *Saniwa ensidens*.

Keywords
Early Eocene; China; Varanidae; Evolution

Introduction
The lizard family Varanidae encompasses more than 80 living *Varanus* species (Auliya & Koch, 2020) currently distributed across Africa, Asia and Australia, and a few close fossil relatives. These lizards have long intrigued both researchers and amateur enthusiasts. Despite having a relatively conservative morphology, *Varanus* is unusual in showing high taxonomic and ecological diversity within a single genus (albeit within several sub-genera, Mertens, 1942; Böhme, 2003), as well as the widest range of body sizes of any extant lizard clade, from 0.12 m to 1.6 m (Snout-vent length [SVL]) (Pianka, King & King, 2004; Auliya & Koch, 2020). In addition to the extant Komodo Dragon (*V. komodoensis*: total length including tail ~3m), *Varanus* also includes the extinct Australian *V. prisca* [=*Megalania*]), the largest known terrestrial lizard with an estimated total length of up to 5 m (Conrad et al., 2012). Among living species, the Bornean Earless Monitor *Lanthanotus borneensis* is the sister taxon to *Varanus* (Conrad, 2008; Gauthier et al., 2012).

There is a general consensus that Varanidae had its roots in Eurasia among the varaniforms (sensu Conrad, 2008, see below) of the Late Cretaceous (Estes, 1983) (Vidal et al., 2012) (Brennan et al., 2021), with several well-preserved fossil varaniforms known from the Campanian deposits of the Gobi Desert (Gilmore, 1943) (Borsuk-Białynicka, 1984; Gao & Norell, 2000) (Norell, Gao, & Conrad, 2007). The origin of the true monitor *Varanus* is more controversial, with Asian, African and Gondwanan origins having been proposed (Brennan et al., 2021).

Many early records of *Varanus* are from the early Neogene of Europe and northern Africa, represented mostly by isolated vertebrae, except *V. rusingensis* (Clos, 1995: Miocene, Kenya), *V. mokrensis* (Ivanov, Ruta, Klembara, & Böhme, 2017: Miocene, Czech Republic), and *V. marathonensis* (Conrad et al., 2012: Miocene, Greece) (Villa et al., 2018: Miocene, Spain) (Figure 3B). The Paleogene temporal gap between the Late Cretaceous varaniforms and the first Neogene records of *Varanus*, is therefore a key period in the evolution of true monitors. However, the only definitive stem-varanid material from this era is that of *Saniwa ensidens*. Although this species is represented by several skeletons from North America (Gilmore, 1928) (Rieppel & Grande, 2007), Paleogene varanid fossils are mostly isolated vertebrae, such as stem-*Varanus* vertebrae reported from the early Oligocene of Egypt (Smith, Bhullar, & Holroyd, 2008) (Holmes et al., 2010), and *Saniwa* vertebrae from the middle Eocene of Mongolia (Alifanov, 1993).

The Paleogene fossil record of varaniforms from China is very poor, with only a dentary and a series of vertebrae (Varaniformes, gen et sp. indet.) reported from the Palaeocene of Qianshan locality, Anhui Province (Dong, Evans, & Wang, 2016). Herein we describe a well-preserved skull and skeleton of a new stem-varanid that was collected in 2008 by a field team of the Paleogene mammal research group of the Institute of Vertebrate Paleontology and Paleoanthropology, Chinese Academy of Sciences (IVPP, CAS), from the Lower Eocene Yuhuangding Formation at the Dajian locality, Liguanqiao Basin, China. This specimen is important in showing that stem varanids were present in Asia as well as Euramerica in the Paleogene.

Geological Background

The lizard specimen, IVPP V 22770, was found at the Dajian locality, which is located about 47.5 km northeast of Shiyan City and lies in Xijiadian Township, Danjiangkou City, Hubei Province (Figure S1). The Liguanqiao Basin, where the Dajian locality occurs, exposes deposits from the Late Cretaceous to Neogene. The Eocene deposits are widely distributed and divided into the Yuhuangding, Dacangfang, and Hetaoyuan formations in ascending order (Ma & Cheng, 1991). The lizard fossil was recovered from the middle one of the three fossiliferous horizons within the Yuhuangding Formation, and is early Eocene in age (Ma & Cheng, 1991) (Wang et al., 2019). There is no absolute dating for the horizon, but the same horizon has yielded abundant mammal remains, including *Rhombomylus turpanensis*, *Advenimus hupeiensis*, *Asiocoryphodon conicus*, and *Danjiangia pingi*, which suggest a late early Eocene age (Ma & Cheng, 1991) (Wang, 1995). The palaeoclimatic conditions below the first fossiliferous horizon in the middle member of the Yuhuangding Formation have been carefully reconstructed based on the presence of the Palaeocene-Eocene Thermal Maximum (PETM), when it was warm and humid with increased precipitation (Zhu et al., 2010) (Chen et al., 2014) (Chen, Ding, Yang, Zhang, & Wang, 2016). However, the locality was within the broad arid belt in the Eocene (Sun & Wang, 2005) although no relevant data has been obtained from the lizard-bearing horizon itself.

Material and Methods

The lizard specimen (IVPP V 22770) is a relatively complete skeleton in which the postcranial elements are mostly disarticulated and scattered in a limited mass within a reddish siltstone block (Figure 1A). The skull, originally preserved in ventral view, was carefully prepared off the main block to expose the dorsal surface and to permit a

high-resolution CT scan (Figures 2, S2, S3). Two articulated trunk vertebrae were also prepared free from the block (Figures S2, S8A) to obtain detailed morphological information and for CT scanning. The specimen is deposited in the collection of the Institute of Vertebrate Paleontology and Paleoanthropology, Chinese Academy of Sciences (IVPP, CAS).

1) High resolution computerized tomography

The skull was scanned twice at the Key Laboratory of Vertebrate Evolution and Human Origins of the Chinese Academy of Sciences (KLVEHO, CAS), once for the whole skull and then again for the braincase. It was then rescanned at the Yinghua Inspection and Testing Centre to yield higher resolution images. The two vertebrae were also scanned at the KLVEHO, CAS to reveal the anatomy of the articulation between the vertebrae. See supplementary Text S1 for the detailed scan parameters. The reconstructed slices were processed in Avizo 9.1 (Thermo Fisher Scientific Inc.) to visualize the slice data and segment the bony elements of interest. Snapshots were then taken from rendered images of the skull, the braincase and the vertebrae. The surface data from several separate fragments of one vertebra was reconstructed in Avizo 9.1 to give a better view of the vertebra as well as to provide more accurate measurements.

2) Histological sections of ribs and fibula

Histological sections were sampled from the mid diaphysis of the right fibula and the proximal parts of two ribs from specimen IVPP V 22770 (Figure S2 for the sample positions). Another section was also made from the distal part of the rib of a commercially obtained specimen of *Varanus*, stated to be *V. salvator*, which was of approximately the same body size (84 mm skull length) as the fossil specimen, and whose astragalocalcaneum still displayed a clear suture. Sections were made using the EXAKT-Cutting-Grinding System at the KLVEHO, CAS (see supplementary Text S2 for the detailed process), and then viewed and photographed using a Zeiss PromoTech microscope.

3) Comparative osteology

Comparative skeletal material of *Varanus* was examined at the Natural History Museum, London (NHM, London) and the Natural History Museum, Basel. These observations were supplemented by digital CT data on the Digimorph website, University of Texas, Austin (http://digimorph.org/index.phtml) and MorphoSource (https://www.morphosource.org), and CT scan data of a *Lanthanotus* specimen in the collections of the Kanagawa Prefectural Museum of Natural History, Japan. A full list of specimens examined can be found in the supplementary Table S1.

4) Nomenclatural usage

For clarity we are using Varanidae in the restricted sense of *Varanus* and those fossil taxa more closely related to it than to *Lanthanotus*. Lanthanotidae is the sister taxon to Varanidae, and encompasses *Lanthanotus* and fossil taxa more closely related to it than to *Varanus* (e.g., *Cherminotus*, Conrad, 2008; Brennan et al., 2021). Varaniformes (sensu Conrad, 2008) encompasses anguimorphs more closely related to *Varanus* than to *Anguis*, *Heloderma* or *Xenosaurus*. We avoid Varanoidea because as used in traditional morphology-based phylogenies this encompasses *Heloderma* as well as *Lanthanotus* and *Varanus*, whereas molecular phylogenies (e.g. Vidal et al. 2012) place *Heloderma* closer to Anguidae (within Neoanguimorpha) than to

varanids. This is important as it suggests morphological characters shared by *Heloderma* (e.g. posteriorly extended – 'retracted' – external narial opening, sharply recurved teeth, broad based teeth with a shallow implantation and plicidentine) and varaniforms have evolved independently and should be treated with caution in comparisons.

5) Phylogenetic analysis

To explore the position of *Archaeovaranus* within Squamata generally, we first coded it into the morphological matrix of Gauthier et al. (2012), and ran two analyses, one unconstrained and one constrained by a molecular backbone (see supplementary Text S3). Having confirmed the placement of *Archaeovaranus* within Anguimorpha, we then coded it into the more focused dataset of Villa et al. (2018), as modified from Conrad et al. (2011), using the character ordering of Conrad et al. (2011) and the matrix amendments of Villa et al. (2018) (see supplementary Text S3 for a detailed explanation). We replaced the coding of '*Saniwa' feisti* in the original matrix with data from the recent redescription of that species as *Palaeonecrosaurus feisti* by Smith and Habersetzer (2021), and we added codings for *Heloderma suspectum* and *Eosaniwa kuhni*. The resulting full matrix had 496 morphological characters, 5729 molecular characters and 88 taxa (OTUs) (supplementary Data S1). *Shinisaurus* was the designated outgroup for four analyses, as it is now considered the sister taxon to *Lanthanotus*+*Varanus* amongst extant squamates (e.g., Pyron, Burbrink & Wiens, 2013), but we also ran four analyses with *Heloderma* as the outgroup.

Parsimony analyses were then conducted in TNT v 1.5 (Goloboff & Catalano, 2016), using the New Technology search with sectorial search, ratchet, drift and fusion options activated (default settings) with a minimum length tree to be found in 20 replicates. Each of the analyses was run with the full combined data set (to ensure the correct positioning of extant taxa), then with the morphological data set alone. In the analyses using only morphological data, we deactivated a subset of taxa represented by mainly molecular data. We also ran the analyses with or without the marine dolichosaur taxa, as there is a lack of consensus as to their position (or that of Mosasauria as a whole) within Squamata (e.g. Gauthier et al., 2012) (see supplementary Text S3 for further explanation).

Systematic Paleontology

Squamata Oppel, 1811
Anguimorpha Fürbringer, 1900
Varanidae Merrem, 1820
Archaeovaranus lii gen. et sp. nov.

Etymology. The generic name Archaeo- reflects the primitive phylogenetic position of this lizard in the evolution of Varanidae, and -varanus suggests the close relationship with the genus *Varanus*, whereas the specific name lii honors the late Prof. Chuankui Li for his important work on Paleogene mammals, including some from the same locality as the holotype lizard described herein.

Holotype. IVPP V 22770, a nearly complete skeleton with an intact skull and associated but mostly disarticulated postcranial elements (Figure 1A).

Locality and Horizon. Dajian locality (IVPP fossil site catalogue number 76006, see Ma et Chen, 1991) (32°46′19.74″N, 111°12′33.06″E), about 35 km northwest of

Danjiangkou City, Hubei Province, China; Middle Member, Yuhuangding Formation (early Eocene; 52~56 Ma; the paleomagnetic study suggesting a precise age of 53 Ma for the fossil-bearing horizon, Jiang et al., 2014) (Ma & Cheng, 1991) (Wang et al., 2019).

Diagnosis. The new genus and species is a medium-sized stem-varanid that resembles *Saniwa ensidens* and *Varanus* and differs from helodermatids, palaeovaranids, lanthanotids, and the Late Cretaceous stem-varanids in combining the following characters: posteriorly extended ('retracted') external narial openings that reach frontals; a single median nasal; two lacrimal foramina, the ventral of which is fully enclosed by the lacrimal; elongated vomers; a U-shaped palatine; a short maxillary tooth row mostly confined to preorbital region, bearing well-spaced recurved teeth with basal plicidentine; intramandibular joint; splenial positioned anterior to level of dorsal prominence of the coronoid; anterior process of coronoid long; and distinct precondylar constriction on the vertebral centra. *Archaeovaranus* resembles *Saniwa ensidens* and differs from *Varanus* in having cristae cranii of frontal separated in ventral midline, separate postfrontal and postorbital, a complete bony postorbital bar, teeth on palatine and pterygoid, posterolaterally placed basal tubera on basioccipital, and a single coracoid emargination. It differs from *Saniwa ensidens* in having a longer rostrum, two pterygoid tooth rows (vs a single row), and resembles *Varanus* but not *Saniwa* in having a dorsal lacrimal foramen enclosed by the prefrontal and lacrimal (rather than being restricted to the lacrimal). *Archaeovaranus* differs from both *Saniwa ensidens* and known species of *Varanus* in having the forelimb and hind limb, and the humerus and femur, of near equal length.

Description

The holotype and only specimen, IVPP V 22770 (Figure 1A), is a nearly complete skeleton, in which the skull is almost intact but the postcranial elements are mostly disarticulated and scattered within the siltstone block. Judging by the visible skeletal growth lines in sections of the right fibula, the animal was probably an adult of about 16 years old at death (see below). However, there is evidence that the animal was still growing. Whereas complete fusion of the long bone epiphyses has occurred at the proximal end of some bones (humerus, femur) it is lacking at the distal ends of the same bones. This asynchronous fusion has also been reported in *Varanus* (de Buffrénil, Ineich, & Böhme, 2004).

The description that follows is based on first-hand examination of the specimen as well as the 3D renders of the skull and sampled vertebrae from the computerized tomography data.

Cranium and Mandibles

The skull is mostly articulated and was preserved on the edge of the block (Figure 1A). During collection in the field, the anterior part of the snout (partial premaxillae, maxillae and vomers) had detached from the rest of the skull but was replaced when the skull was prepared off the block (the missing part is very limited, and the distance between the snout tip and the rest of the skull was estimated based on the shape of the vomer and premaxillary nasal process). The left side of the skull was already broken when the skeleton was recovered; the left palpebral bone, jugal, postorbital, parietal, pterygoid and paroccipital process are partly broken, and the squamosal and supratemporal bones are completely missing. The left quadrate was detached from the

skull and lay among the postcranial elements (Figure 1B). The two lower jaws are in articulation at the symphysis but are slightly displaced from the cranium. The left mandible preserves only the dentary and the coronoid *in situ* in lateral view; the displaced postdentary elements are partially preserved in medial view and located below and left of the skull (Figure 1A). There is a section missing from the postdentary region (Figure S4D). The right mandible is preserved in medial view and is nearly complete, with the retroarticular process missing (Figures 1A, S4A). Neither of the mandibles could be removed from the block for scanning as this would have damaged the adjoining bones.

Cranium. The cranium (Figures 2, S3) is depressed dorso-ventrally, even allowing for some taphonomic compression. The skull roof is generally smooth except for an area of vermiform or "worm-like" sculpture around the frontoparietal suture (Estes, Queiroz, & Gauthier, 1988). The mid-frontal suture is raised into a ridge that continues onto the parietal, up to the parietal foramen. The snout is elongated, but not strongly tapering, and the external narial openings are posteriorly extended ('retracted') so that the nasals and prefrontals are fully separated and the frontal enters the external narial margin. This resembles the condition in *Varanus* and *Saniwa ensidens*, but the external narial opening barely reaches the frontal in *Lanthanotus*, and fails to reach it in *Ovoo* (Norell, Gao, & Conrad, 2007), *Paranecrosaurus* (Smith & Habersetzer, 2021), or *Heloderma*. The orbit is closed posteriorly by the jugal and postfrontal. The borders of the supratemporal fenestra are completed laterally by the postorbital and squamosal. The braincase is largely exposed in dorsal view (Figures 2A, S3B). As in *Varanus*, the tooth row is almost confined to the preorbital region, with the last maxillary tooth at or only slightly beyond the anterior extremity of the orbit (Figure 2C). In ventral view, the palate is fully neochoanate, with the vomeronasal opening completely separated from the choana. The suborbital fenestra is moderate in size, and the maxilla was excluded from the borders of the fenestra. The interpterygoid vacuity reaches anteriorly at least half way between the vomers, and it gradually widens posteriorly. No trace of cranial osteoderms is preserved on the specimen.

The single premaxilla (Figures 2, S3, S5A) is complete. Four pointed pleurodont teeth are preserved along its alveolar border, but allowing for empty alveoli, the original premaxillary tooth count was probably eight (7-9 in *Varanus*, see Evans, 2008). A long nasal process arises from the alveolar lamina and extends posteriorly rather than posterodorsally. A small foramen for medial ethmoidal branches of ophthalmic and ethmoidal nerves and the ethmoidal artery (Bellairs, 1949) perforates the base of the nasal process on each side, as in *Saniwa ensidens* (Rieppel & Grande 2007), but there is no sign of the foramina often present on the antero-dorsal surface of the alveolar lamina as in *Varanus*. In dorsal view, the nasal process is moderately broad, and only slightly dilated where it contacts the nasal. The process extends to, or just beyond, the midpoint of the external narial openings, forming the anterior half of the internarial bar, but it does not meet the frontals below the nasals. The process is roughly triangular in transverse section anteriorly, but becomes T-shaped posteriorly with the vertical ventral lamina sandwiched between the two anterior laminae of the nasals. The tapering posterior tip of the process is again triangular in cross section and is supported from below by the already fused nasals. The palatal plate of the premaxilla is well-developed and divides posteriorly into two processes, each of which meets the maxilla and the anterior end of the vomer. The palatal plate bears an anteromedian

incisive process composed of two crescentic halves. Laterally, the premaxilla is slightly overlapped by the premaxillary process of the maxilla, enclosing a small premaxillary-maxillary aperture.

The right maxilla (Figures 2C, S5B) is almost complete, whereas the left one (Figure S3D) has lost much of the alveolar plate as well as the teeth. The maxilla, in general, is long, low, and subtriangular in shape. The long premaxillary process is horizontal and gradually broadens anteriorly as seen in dorsal view. The anteromedial margin of the process is slightly concave, and contributes to the formation of a small premaxillary-maxillary aperture. There is a triangular depression on the dorsal surface of the premaxillary process, with distinct lateral and more pronounced medial ridges. The medial ridge forms a lateral support for the septomaxilla, and is perforated posteromedially by a foramen for the maxillary nerve and artery (Bellairs, 1949). Further posteriorly, the maxilla expands very gradually, forming the oblique anterodorsal margin of the facial process. The low facial process curves inwards and contributes to the skull roof, with the horizontal posterior tip well separated from the nasal and the frontal by the prefrontal. Although Rieppel and Grande (2007) thought the medial curvature of the facial process differentiated *Saniwa ensidens* from *Varanus*, a similar curvature does occur in some *Varanus* species (e.g., *V. prasinus*, UF-H-77411; *V. flavescens*, Mertens, 1942), and the facial process can extend further medially and posteriorly to approach the frontal (some *V. niloticus*, e.g., BMNH 97.5.31.2). The posterior margin of the facial process is more steeply inclined than the anterior one, and bears a small projection at the level of the prefrontal - lacrimal suture. A similar projection is located in this position in some *Varanus* (*V. salvator*: BMNH 1972.2160; *V. bengalensis*: BMNH 1974.2479), but not all species (e.g., *V. gouldii*: BMNH 1983.1132). The facial process overlaps the prefrontal extensively, as well as a small portion of the lacrimal. The posterior jugal process is short, with all but the last maxillary tooth positioned anterior to the orbit. This contrasts with *Saniwa ensidens* in which, two or three maxillary teeth have a suborbital position (Rieppel & Grande, 2007). In ventral view, the maxillary palatal shelf is well-developed anteriorly, narrows gradually into a low medial ridge posterior to the midpoint of the maxilla, and then expands slightly where the maxilla meets the palatine. The broad anterior part of the shelf flares ventrally and may originally have met or almost met its counterpart in the midline. Just behind the anteromost articulation with the vomer, there is an additional contact between the maxillary palatal shelf and the vomer, separating the vomeronasal fenestra from the choana (neochoanate palate). Posteriorly, the maxilla is excluded from the margin of the suborbital fenestra by the contact of the palatine and ectopterygoid, as in *Varanus*, *Lanthanotus*, and *Saniwa ensiden*s, but also *Palaeoenecrosaurus feisti* (Smith & Habersetzer, 2021) and *Heloderma*. Dorsal to the palatal shelf, the opening of the infraorbital canal, for the nervus alveolaris superior and maxillary artery (Bellairs, 1949), lies at the anterior extremity of the maxillary - palatine articulation; posterior to this articulation, the maxilla contacts the jugal and ectopterygoid.

Both septomaxillae (Figures 2, S3, S5C) are preserved *in situ* but had lost a small medial portion. Each bone is roughly triangular in shape. It is ventrally concave but shallow, to accommodate Jacobson's organ (vomeronasal organ), and its dorsal surface is flattened and smooth, with a prominent process arising close to the anteromedial border of the bone that extends antero-laterally beyond the septomaxillary - maxillary suture. The septomaxilla is extremely complicated in some

Varanus (for example, *V. exanthematicus*) with additional fenestrate laminae and spikes on the dorsal surface. In IVPP V 22770, the medial margin thickens to accommodate a canal for the medial ethmoidal branch of the ophthalmic and ethmoidal nerves (trigeminal nerve branches) and the ethmoidal artery, as in *Lanthanotus* (YPM 6057, digimorph; Evans' Lab, CT data of Kanegawa Prefectural Museum of Natural History specimen). This region varies in *Varanus*, from being open dorsally (*V. acanthurus*, *V. salvator*, *V. prasinus*), to forming a medial groove (*V. komodoensis*, *V. mokrensis*). The septomaxilla of *V. bengalensis* has a nearly closed canal (Bellairs, 1949) that extends along the posterior two-thirds of the medial margin, but opens dorsally as a shallow groove further anteriorly. The septomaxilla is supported by the vomer in some *Varanus* species (for example, *V. exanthematicus microsucus*, *V. prasinus*, *V. komodoensis*), but this articulation is not present or preserved in *Archaeovaranus*.

The nasal (Figures 2, S3 S5D) is long and unpaired, as in most *Varanus*, *Saniwa ensidens* and *Lanthanotus*, but not *Ovoo* (Norell, Gao, & Conrad, 2007) nor *Palaeonecrosaurus* (Smith & Habersetzer, 2021). It is complete except for the posterior tips, but the facet on the frontals shows where the nasal ended. The anterior end appears to bifurcate into separate laminae that diverge slightly to form a narrow dorso-median slot for the tapering nasal process of the premaxilla. However, the laminae are soon fused ventrally to form a shelf that underlies the process posteriorly. The nasal is of consistent width in its anterior three-fifths, but at its contact with the frontals, the nasal widens and then bifurcates. Each of the posterior nasal processes invades the anterior border of the corresponding frontal, and extends beyond the posterior margin of the external narial opening. The nasal does not contact either the prefrontal or maxilla, leaving the frontal to form the posterior margin of the external narial opening. In ventral view, a low midline ridge shows the line of fusion of the originally paired nasals. The nasal is relatively long, even by comparison with most living *Varanus* species.

The frontals (Figures 2, S3, S5F) are paired, and their medial margins thicken slightly to form a low dorsal ridge along the median suture. Other than this ridge, also seen in *Saniwa ensidens* (Rieppel & Grande 2007), and a slightly posteromedial rugosity, the frontal is smooth. As in *Varanus* and *Saniwa ensidens*, the anterior margin of each frontal supports the nasal from below and bears both an anteromedial process and a much longer anterolateral process. The frontals widen slightly from the anterior margin to the level at which their lateral margins enter the orbit. The orbital borders are then parallel for a short distance before expanding at the frontoparietal suture to roughly twice the interorbital width. The cristae cranii (*sensu* Oelrich, 1956) or subolfactory crests are moderately developed but remain well-separated in the midline, unlike those of *Varanus*, *Ovoo gurval* (Norell, Gao, & Conrad, 2007), and also *Heloderma*, that meet, or nearly meet (for example, the fossil species *V. mokrensis*; Ivanov et al., 2017), in the midline below the olfactory tracts. Anterior to the orbit in *Archaeovaranus*, the crests gradually reduce in depth and do not contribute to the orbitonasal septum (i.e., the septum is composed only of the prefrontal orbitonasal flange). Further posteriorly, each crest ends abruptly where the frontal starts to expand. Anterolaterally, a large, triangular prefrontal facet invades the crest and extends posteriorly over two-thirds of the frontal length; a much smaller postfrontal facet lies at the posterolateral margin of the frontal. The prefrontal, together with the postfrontal, strongly limits, but does not exclude, the contribution of

the frontal to the orbital margin, as in most *Varanus* (except in some old individuals of, for example, *V. komodoensis* and *V. exanthematicus*). The frontoparietal suture is transverse and nearly straight. The structure of this suture is variable in *Varanus*, and it is interdigitating in *V. mokrensis* (Ivanov et al., 2017). Dorsal facets are present on the frontals of *Archaeovaranus*, albeit very small, to support a corresponding anterolateral lappet from the parietal. This tab is commonly present in *Varanus*, and it is weak in *Lanthanotus*. According to Rieppel and Grande (2007), *Saniwa ensidens* lacks an anterolateral parietal lappet and the corresponding facet on the frontal.

The parietal (Figures 2, S3, S5G) is nearly complete, with only the left postparietal process (supratemporal process) missing. A parietal foramen is present and positioned in the anterior quarter of the parietal table. There is a ridge anterior to the parietal foramen, which is also present, in *Saniwa ensidens* (Rieppel & Grande 2007) and in some specimens of *Varanus* (for example, *V. prasinus* UF-H-71411). The parietal table is longer than wide and is strongly constricted in its mid-section. It is widest at the frontoparietal suture (nearly twice that of the mid-section) and widens only slightly at the posterior end, before the postparietal processes diverge. The parietal table slightly overhangs the ventrolateral flange (cristae cranii parietalis) in its anterior half, to form a fossa that accommodates the postfrontal facet. There is no alary or epipterygoid process on the flange, but a small posterior surface suggests it may have met the prootic. The postparietal processes are about the same length as the parietal table, and diverge posterolaterally at an angle of around 90˚. These processes are lamina-like, with the lamina horizontally oriented at its base but vertically oriented distally at the articulation with the supratemporal. The supratemporal facet extends along more than half the lateral surface of the postparietal process. The process tapers in its distal quarter, so that the ventral margin of the supratemporal bar is formed by the supratemporal bone which separates the parietal from the squamosal, as in *Varanus*, *Lanthanotus*, and also *Heloderma*. However, the supratemporal does not extend on to the medial surface of the postparietal process. At its distal end, the process fails to reach the paroccipital process of the otooccipital, unlike *Lanthanotus*, *Heloderma*, and most *Varanus* where there is a small contact. In occipital view, little or no nuchal crest is evident, but there are small, shallow nuchal fossae on each side of the midline. The pit for the ascending process of the supraoccipital (processus ascendens) is located anterior to the posterior margin of the parietal table (invisible in dorsal view), and opens posteriorly.

Seen in dorsal view, the prefrontal (Figures 2A, S3B) is an elongate, strap-like bone, but it is more or less triangular in lateral view. Its anterior lamina is longer than deep, and extends more anteriorly than antero-ventrally (Figure S5E), so contributing more to the roof than the lateral wall of the nasal cavity. This feature is variable in *Varanus*. For example, the prefrontal morphology of *Archaeovaranus* is similar to that of *V. komodoensis*, but differs from that in the deep skull of *V. exanthematicus* where the anterior lamina extends ventrally and contributes only to the lateral wall of the nasal cavity. Anteriorly, a portion of the anterior lamina is overlapped by the facial process of the maxilla. The medial margin of the anterior lamina partially contributes to the margin of the external naris. The orbitonasal flange is broad and its concave ventral margin sutures with the palatine across its width (Figure S5E). The medial margin of the flange is vertical and borders the orbitonasal passage. Laterally the prefrontal is sutured to the lacrimal, and together they enclose the more dorsal of the two lacrimal foramina. Dorsally, the tapering posterior frontal process is triangular in section and

extends beyond the two-thirds of the frontal. At the level of the orbitonasal flange, it supports the palpebral bone.

Well-developed palpebral bones (Figures 2A, S3B) are preserved on both sides although the posterior tip of the left bone is broken. The broad anterior base attaches to the prefrontal, in the anterodorsal corner of the orbit. The presence of an anterolateral process, as in most *Varanus* species but not, apparently, in *Saniwa ensidens* (Rieppel & Grande, 2007), cannot be confirmed. The posterior process extends straight backwards beyond the midpoint of the orbit. Palpebrals are present, but small, in *Lanthanotus* and absent in *Heloderma*, but they are well-developed in the palaeovaranid *Palaeonecrosaurus feisti* (Smith & Habersetzer, 2021).

The lacrimal (Figures 2C, S3) is of moderate size. In lateral view, it is triangular and longer than deep, unlike most *Varanus* where the exposed lacrimal is deeper than long (Bellairs, 1949). The lacrimal is overlapped by the maxilla and the jugal anteroventrally, and it bears a small posterior projection, as in some species of *Varanus*. As in *Varanus*, there are two lacrimal foramina positioned one above the other. As noted above, the dorsal foramen appears to be enclosed by the lacrimal and prefrontal, whereas the slightly smaller ventral foramen is fully enclosed by the lacrimal itself, the same arrangement as found in *Varanus* and the Late Cretaceous Mongolian *Ovoo* (Norell, Gao, & Conrad, 2007). In all *Varanus* species, the dorsal duct (and therefore its foramen) is larger than the ventral one, but the relative disparity in size of the two foramina varies considerably (Bellairs, 1949). In *Saniwa ensidens* both lacrimal foramina are fully enclosed by the lacrimal (Rieppel & Grande, 2007), but there is disagreement (or variation) about the condition in *Lanthanotus*. Rieppel and Grande (2007) wrote that both foramina lie at the prefrontal-lacrimal border, and the description in McDowell and Bogert (1954) implies the same thing. Moreover, this does appear to be the condition in FMNH148589 (The Deep Scaly Project, 2011). However, Norell, Gao and Conrad (2007) stated that both foramina perforate the lacrimal in *Lanthanotus*, so there may be variation. The lacrimal foramen is single in palaeovaranids (Smith & Habersetzer, 2021) and in *Heloderma*.

The right jugal is complete whereas the left one only preserves its anteroventral suborbital ramus (Figures 2, S3). The bone is long, slender and angulate (Figures 2C, S3E, S6F). The anterior suborbital ramus is relatively deep and bilaterally compressed. Its anterior tip meets the lacrimal and palatine to exclude the maxilla from the orbital margin. Further posteriorly, the jugal articulates with the ectopterygoid medially and ventrally, with the ectopterygoid facet forming a low longitudinal ridge. The lateral surface of the suborbital ramus is smooth and is perforated by a line of three foramina. Posterior to the ectopterygoid articulation, the jugal angles dorsally into a rod-like postorbital ramus. This ramus articulates with the postorbital bone to complete the postorbital bar. The jugal does not contact the postorbitofrontal bone in most *Varanus* and varies in size from a splint-like suborbital element in *V. prasinus*, to a more extensive element that almost contacts the postorbitofrontal in large *V. griseus* (BNHM 1974.2418). Although Gilmore (1928) could not determine whether the jugal and postorbital met to form a complete bar in his specimen of *Saniwa ensidens* (USNM 2185), and Rieppel and Grande (2007) were also unable to reach a firm conclusion on this point, the shape of the jugal in both

USNM 2185 and FMNH PR2378 suggests that the postorbital bar was probably completed by the jugal in those specimens.

The postfrontal and the postorbital (Figures 2, S3B) are separate on both sides of the skull in *Archaeovaranus*. Taken together, the two bones are similar in shape to the (usually) fused postorbitofrontal bone in *Varanus*. Moreover, the shapes of the individual postfrontal and postorbital in IVPP V 22770, are similar to those in a hatchling *Varanus panoptes* (Werneburg, Polachowski, & Hutchinson, 2015), where the bones have not yet fused. In dorsal view, the postfrontal (Figures 2A, S3B) appears triradiate, and two medial rami, of about the same length, embrace the lateral margins of the frontoparietal junction. However, linking the two medial rami there is a prominent ventral lamina that supports the frontoparietal suture from below. This lamina is only rarely developed in *Varanus* species such as *V. komodoensis* and is absent in *Lanthanotus*. The anterolateral ramus of the postfrontal is short and extends anteriorly together with the anterior process of the postorbital, almost reaching the jugal. The fourth ramus, a small posterolateral projection that is entirely obscured by the postorbital, supports the postorbital ventrally (Figure S6B). The postorbital (Figures 2A, S6C) is an elongate and dorsoventrally depressed element. The bone is robust, being widest just posterior to the articulation with the postfrontal. Anteriorly, the bone narrows into a knob-like anterior process that is inserted between the anterolateral process of the postfrontal and the jugal in dorsal view, completing the postorbital bar. Posteriorly, the bone tapers gradually and articulates with the squamosal from above. It extends posteriorly beyond the midpoint of the supratemporal fenestra.

The postfrontal and postorbital are fused in one articulated skeleton of *Saniwa ensidens* (FMNH PR2378, Rieppel & Grande, 2007), but are unfused in the holotype (Gilmore, 1928). The two bones are usually fused in adult *Varanus*, but a recent study of skull ontogeny in *Varanus panoptes* confirmed that the postfrontal and postorbital originate separately during embryonic development and, at least in this species, fuse together very early (Werneburg, Polachowski, & Hutchinson, 2015). However, Mertens recorded finding examples of separate postfrontal and postorbital bones in adults of many species of *Varanus* (Mertens, 1942), and considered this to be a variable character without taxonomic significance.

The right squamosal (Figures 2A, S3B) is complete except for its anterior tip, but the shallow squamosal facet on the right postorbital suggests the squamosal almost reached the anterior margin of the supratemporal fenestra, as in *Varanus* and *Saniwa ensidens*, but not *Lanthanotus* or *Heloderma* where the squamosal is reduced. The bone (Figure S6E) is dorsoventrally compressed at its articulation with the postorbital anteriorly, and mediolaterally compressed where it meets the supratemporal bone posteromedially. The posterior end of the squamosal curves ventrally and terminates as a knob. Together with the supratemporal and the paroccipital process of the braincase, the squamosal suspends the quadrate.

The supratemporal bone (Figures 2C, S3E, S6D) forms a deep and slightly curved lamina. It fits into the facet on the lateral surface of the postparietal process for about half the length of that process. Further posteriorly, the supratemporal wraps under the ventral margin of the postparietal process but does not invade its medial side. At its

posterior tip, the supratemporal protrudes beyond the postparietal process, and is sandwiched between the paroccipital process and the squamosal.

The left quadrate is preserved between the left pterygoid and squamosal (Figures 2C, S6A); the right quadrate is displaced from the skull and its ventral condyle is missing (Figure 1B). The dorsal part of the central pillar is curved posteriorly and thus the dorsal condyle faces both dorsally and posteriorly. The posterolateral concha bears a shallow to moderately developed concavity that is bordered laterally by a tympanic crest. The structure of the quadrate is within the range of variation of *Varanus*, although the medial lamina is more developed than in *Varanus*. The dorsal condyle is rounded, suspended by the supratemporal, squamosal and paroccipital process as described above, but there is no obvious notch between the condyle and the tympanic crest. The mandibular condyle is large and saddle-like, with the medial half larger than the lateral half.

The vomers (Figures 2B, S3A, S6G) are elongated and narrow as in *Varanus*. Each has a slightly expanded anterior tip that meets the premaxilla and maxilla, but the anterolateral vomerine margin is notched before expanding into a short flange that met the palatal shelf of the maxilla to enclose the vomeronasal opening (neochoanate palate). In ventral view, the median recess for the palatal sinus is flanked by prominent ventral ridges (Figure S6G1). The dorsally open gutter (supravomerine canal in Rieppel, Gauthier, & Maisano, 2008) is wide and deep for almost its entire length, as in *Varanus salvator*. The gutter is said to be broader and deeper in *Saniwa ensidens* than in *Varanus* (Gilmore, 1922). In some *Varanus* (*V. komodoensis*, *V. prasinus*, *V. acanthurus*), the lateral wall of the gutter is much more developed than its medial wall. The two vomers diverge posteriorly to a small extent, leaving the interpterygoid vacuity extending anteriorly for slightly less than half of the vomer length. This is similar to the condition figured in the Cretaceous *Ovoo gurval* (Norell, Gao, & Conrad, 2007). The vomers in *Saniwa* are in contact medially throughout most of their length (Gilmore, 1922), but variable degrees of divergence are seen in *Varanus*, *Lanthanotus*, and *Heloderma*. Posteriorly, the vomer meets the slender anterior process of the palatine in a loose, slot-like joint. One short process passes ventral to the anterior tip of the palatine and one much longer process lies dorsal to the palatine and extends more than halfway across the anterior vomerine ramus of the palatine.

The palatine (Figures 2B, S6H) is short and triradiate with little or no choanal fossa. There seem to have been two rows of palatine teeth, as evidenced by two edentulous ridges (Figure S4B), with one remnant tooth on the right palatine and highly dense tooth-like structures on the CT slices where the palatine teeth should have been. The anterior vomerine ramus is bar-like and articulates with the vomer as described above. The lateral maxillary ramus is greatly expanded, to a greater degree anteriorly than posteriorly, and has a long lateral suture with the maxilla. This ramus also meets the ectopterygoid at its posterior tip to exclude the maxilla from the margin of the suborbital fenestra. A large superior alveolar canal is clearly present (Figure S6H), as in all *Varanus*. The posterior pterygoid ramus is broader but shorter than the anterior vomerine ramus, turning ventrally to articulate with the pterygoid in an interlocking joint. Dorsally, at the junction of the vomerine and maxillary rami, the palatine bears a ridge that meets the orbitonasal flange of the prefrontal.

The pterygoid (Figures 2B, S6J) is triradiate with a broad Y-shaped palatal plate and a long, slender posterior quadrate process. There are two rows of teeth along the raised medial border of the palatal plate and these extend onto the anterior palatine process. The pterygoid flange extends anteroventrally, and bears an articulation facet for the ectopterygoid medially and dorsally. Ventral to the concavity for the basipterygoid process, just posterior to the palatal plate, there is a well-developed medially extending shelf. The quadrate process is roughly triangular in section for half of its length, and then becomes laminar with a longitudinal shallow groove along the medial surface. Its posterior end is pointed and would have articulated with the quadrate in a loose joint. In dorsal view, at the level of the basipterygoid joint, the deep fossa columellae for the articulation of the epipterygoid is visible.

The ectopterygoid (Figures 2B, S3A, S6I) runs roughly anteroposteriorly. It is weakly curved and twisted at the midpoint. Anteriorly the ectopterygoid articulates with the maxilla and the palatine as in *Varanus*, *Lanthanotus*, *Heloderma*, *Ovoo* (Norell, Gao, & Conrad, 2007) and *Saniwa* (Rieppel & Grande, 2007), and with the jugal dorsally. The posterior end diverges into dorsal and ventral processes that clasp the pterygoid from the medial and dorsal sides.

The epipterygoid (Figures 2, S3) is a rod-like element, as in all lizards, with both ends slightly expanded. The right one is preserved *in situ*, fitting into the fossa columellae of the pterygoid ventrally and articulating with prootic dorsally. The left epipterygoid is disarticulated and displaced below the parietal. The orientation of the epipterygoid can be considered as vertical at rest.

There is no sign of an orbitosphenoid in the CT slices, but we cannot be sure whether or not an ossified element was present due to the slight disarticulation in this region.

The braincase (supraoccipital, basisphenoid with parasphenoid, basioccipital, prootic, otooccipital) was well preserved except that the left paroccipital process of the otooccipital is missing. The braincase is exposed in dorsal, ventral and occipital view in the specimen (Figures 2, S3), and the anatomical observations are supplemented by the CT scan data. The CT scan shows that existing cavities in the braincase (such as the otic capsule) contain crystals that blur neighbouring structures due to their strong reflective properties. As a result, the sutures between elements, especially those parts within the matrix, are difficult to discern and the braincase has been segmented as a single structure (Figures 2D, 2E, S7). The presence of foramina has been checked on both sides, as well as on the original scan slices for confirmation. The braincase contacts the parietal via 1) the ossified ascending process of the supraoccipital and 2) the anterodorsal tips of the alar processes of the prootics. There are no additional contacts lateral to the midline between the supraoccipital and the parietal. No stapes is preserved in situ, nor identified within the block.

The braincase floor, as a whole, is elongate (Figures S3A, S7A). The basioccipital is roughly rectangular in ventral view, and narrows abruptly into a small, rounded occipital condyle. In ventral view, the basisphenoid-basioccipital suture (Figures 2B, S7A) is an inverted V-shape with a flat vertex, terminating laterally at the apices of the basal tubera. Norell and Gao (1997) described the basisphenoid and basioccipital suture in *Estesia mongoliensis* as strongly arched anteriorly, which is very similar to the “obtusely angulate suture” noted by McDowell & Bogert (1954) in basal

anguimorphs, and also present in *Heloderma*, but different from the straight-line suture in *Varanus* and *Lanthanotus*. This suggests that *Archaeovaranus* retained the primitive state. The basal tubera are well-developed, although the epicondyles are not preserved, and they are positioned posterolaterally, with their basioccipital apex just behind the base of the prootic-opisthotic suture (Figure 2E). In *Lanthanotus* and *Varanus*, the basal tubera are positioned anteromedial to the prootic-opisthotic suture, with their apices at the lateral junction of the sphenoid and basioccipital; they lie further posteriorly in *Heloderma*. As in some *Varanus* species (e.g., *V. griseus*), the tubera of *Archaeovaranus* extend both laterally and ventrally, such that the crista tuberalis slopes dorsally. However, in other *Varanus* species (e.g., *V. salvator*), the tubera just extend laterally and the crista tuberalis is almost horizontally positioned. The dorsal surface of the crista tuberalis is excavated by the occipital recess.

The sphenoid (Figures 2D, S7A) is a composite of the basisphenoid and dermal parasphenoid. The parasphenoid is firmly fused to the basisphenoid, leaving no trace of the suture between them. The sphenoid (Figure 2B, S7A) is narrowest just posterior to the basipterygoid processes, but then expands to form a pair of prominent processes that diverge postero-ventrally to reach the basal tubera (see above). Anteriorly, the basisphenoid bears a pair of robust basipterygoid processes which are short but greatly expanded distally. The medial margin of each process is deflected dorsally and forms a dorsally upturned projection that would have increased the articular surface for the pterygoid. The two basipterygoid processes diverge at an acute angle (about 60 degrees) and the bases of trabeculae cranii are located between them, supported from below by an ossified parasphenoid rostrum. The parasphenoid rostrum is slender and extends anteriorly well beyond the anterior termination of the basipterygoid processes. Dorsal to the bases of the two trabeculae cranii (Figure 2D) lies the hypophysial fossa into which the internal carotid foramina open. The two foramina are positioned close to each other and to the braincase floor. Lying between the base of each trabeculum and the corresponding basipterygoid process is the anterior opening of the vidian canal which is almost aligned with the internal carotid foramen. The foramina for the abducens nerves (CN6) are located further dorsally on the dorsum sellae, dorsolateral to the anterior openings of the vidian canal. The abducens foramina are also visible in dorsal view. The dorsum sellae is deep and the alar process of the sphenoid is well-developed, giving the crista sellaris a concave dorsal margin. The alar process protrudes anteriorly and downward, and together with the anterior inferior process of the prootic, partially enclosed the notch (incisura prootica) for the trigeminal nerve. Laterally the entry foramen for the vidian canal lies just posterior to the base of the basipterygoid process, and well below the prootic-basisphenoid suture (Figure 2E) as in *Lanthanotus* and most *Varanus* (such as *V. salvator*), although in *V. exanthematicus*, the posterior opening of the vidian canal is located closer to the prootic-basisphenoid suture. In *Heloderma*, the entry foramen is further posteriorly positioned.

The supraoccipital (Figure S7B, S7C) is well preserved, and is nearly completely exposed in dorsal view. There is a low sagittal ridge on the dorsal surface that is continuous anteriorly with the ascending process. Evans (2008) described the supraoccipital in *Varanus* as having a steeply inclined posterodorsal surface with a variably developed median crest, but this is not always the case in *Varanus*. Anteriorly the ascending process inserts into a posteriorly opening pit in the parietal. The posterior margin of the supraoccipital, forming the dorsal margin of the foramen

magnum, is gently curved as in most *Varanus* and *Shinisaurus* (but angulated in *Lanthanotus*). In *Saniwa ensidens*, it is described as angulated (Rieppel & Grande, 2007) but, based on their figure, the angulation is not prominent and could be an artifact of preservation. The cranial opening of the endolymphatic duct is not discernible on the CT model due to the presence of crystals in that area.

The lateral wall of the ossified braincase (Figure 2E) is mainly made up of the prootic and the otooccipital which enclose the rounded fenestra ovalis. The fenestra lies immediately above the dorsoventrally elongate lateral opening of the recessus scalae tympani in the otooccipital. The two openings are separate by a well-developed crista ventrolateralis that is horizontally positioned. A long posterior process of the prootic extends onto the otooccipital, but its extremity is well-separated from the posterolateral end of the paroccipital process.The prootic bears a moderately developed prootic crest, and an undivided facial foramen lying just below the prootic crest, posterior to the base of the alar process of the prootic. The division of the facial foramen is variable in *Varanus* (Head, Barrett, & Rayfield, 2009). A divided facial foramen was reported for *Lanthanotus borneensis* (Rieppel, 1983; Conrad et al., 2012), but an undivided foramen was observed in the CT scan of the Kanagawa Museum specimen. The condition is not known for *Saniwa*. The anterodorsal alar process of the prootic is well developed as a subrectangular projection. At its tip it meets the weakly developed lateral descending flange of the parietal, and laterally it supports the dorsal head of the epipterygoid. The anterior inferior process is smaller than the alar process of the sphenoid, and together with the anterodorsal alar process, forms the trigeminal notch. In medial view, there seems to be a low medial ridge at the base of the prootic alar process, but there is no supratrigeminal process. The presence of a medial ridge and/or a supratrigeminal process is variable in *Varanus*. A faint ridge is present in *V. exanthematicus* (FMNH-58299, digimorph), but was absent in other *Varanus* studied herein (*V. salvator*, *V. komodoensis*, *V. acanthurus*, *V. prasinus*). The medial acoustic recess contains the internal facial foramen and foramina for the vestibulocochlear nerve.

The paroccipital process of the otooccipital in *Archaeovaranus* is well-developed and extends postero-laterally. Its length and orientation are variable in *Varanus*, ranging from a long, posteriorly oriented process in *V. komodoensis* to the short, nearly laterally directed one in *V. salvator*. In *Archaeovaranus*, the ventral margin of the paroccipital process continues ventrally towards the basal tubera and, together with the exoccipital, forms the occipital surface of the braincase (Figure S7C). In occipital view, this ventrolateral margin of the otooccipital is deeply notched to form a prominent ventral process (black arrow in Figure S7C), a condition that differs from that in *Varanus*. A large vagus foramen opens on to the occipital surface lateral to the foramen magnum. Two hypoglossal foramina perforate the exoccipital internally and exit via the vagal canal, a condition similar to that in *Saniwa* (Rieppel & Grande, 2007). There is only one internal hypoglossal foramen in *Lanthanotus*, and it does not exit via the vagal canal, but opens on the medial margin of the vagus foramen. The condition in *Varanus* may be variable as both one and two internal foramina have been reported (Evans, 2008). The vagus foramen lies further ventrally in *Varanus* and *Lanthanotus* than in *Archaeovaranus*, being below the level of the dorsal margin of the exoccipital condyle.

The occipital condyle (Figure S7C) is composed of the basioccipital and exoccipitals, with the basioccipital making a slightly larger contribution. The exoccipitals do not meet to exclude the basioccipital from the dorsal margin of the occipital condyle.

Mandible. As in *Varanus* and *Lanthanotus*, but not *Heloderma*, the lower jaw (Figure 1A, S4A) of *Archaeovaranus* is characterized by a reduced articulation between the anterior dentary unit (dentary, splenial, and coronoid) and the posterior articular unit (surangular, prearticular, articular). No angular was observed. This intramandibular articulation is visible in the right mandible but is also evidenced by the fact that the articular unit of the left lower jaw has separated from the dentary unit.

The dentary, forming roughly half the length of the mandible, is slender and tapers anteriorly (Figure S4A). Its lateral surface is perforated by a line of at least six neurovascular foramina. Posteriorly the dentary seems to bifurcate, if the posterior notch is natural. The subdental shelf is broad but there is no subdental ridge. The meckelian fossa is open ventrally along its anterior half but is covered posteromedially by the splenial and coronoid. The intramandiblar septum is probably obscured by the coronoid and the prearticular in the medially exposed right mandible.

The left splenial is exposed in internal view and may be complete, but it is obscured by the dentary except along the ventral margin (Figure S4A). Adjacent to the right lower jaw is a thin lamina of bone that might, by its length, be the right splenial. The splenial extends anteriorly beyond the midpoint of the dentary. By the impression on the inner surface of the preserved right lower jaw, the posterior extremity of the splenial did not extend beyond the dorsal prominence of the coronoid. No other detail is visible.

The coronoid (Figure S4A) is long and low. The anterior process runs along the dorsal margin of the surangular to clasp the coronoid process of the dentary between medial and lateral laminae, as in *Varanus* and *Saniwa ensidens*, but also *Heloderma*. The medial lamina is expanded (Figure S4A) and extends forward to enclose the anterior mylohyoid foramen together with the splenial, as in *Varanus*, *Lanthanotus* and *Heloderma*. A low ridge originating from the ventral margin of the lateral lamina extends posterodorsally towards the dorsal prominence of the coronoid bone, creating a posterior depression for attachment of the adductor mandibulae externus superficialis (Oelrich, 1956). A posteromedial process is preserved on the right lower jaw, partially obscured by a rib fragment. It extends ventrally and posteriorly, possibly forming the anterior margin of the adductor fossa.

The right and left postdentary (articular) units (Figures S4A, S4D) are both preserved in medial view, but the region of the adductor fossa is missing from the left lower jaw. On the right mandible, the adductor fossa is small, enclosed by the surangular dorsally and the prearticular ventrally. The surangular extends anteriorly to reach the coronoid anteromedial process. The dorsal margin of the surangular becomes thicker posteriorly. The prearticular is fused with the articular, and is long enough to exceed the level of the anterior tip of the coronoid as preserved. The prearticular is wider than the surangular in medial view anterior to the adductor fossa and bears no angular process. The retroarticular process is preserved on the left side (Figure S4D). It widens posteriorly to become subrectangular but is slightly medially deflected. A shallow retroarticular fossa appears to have been present.

Dentition. The marginal dentition, including the premaxillary, maxillary and dentary teeth, is characterized by the presence of plicidentine (Figure S4C), as in *Varanus* and *Saniwa ensidens*, but also *Heloderma* and possibly *Ovoo* (Norell, Gao, & Conrad, 2007). The teeth are highly pleurodont and expanded strongly at the base (i.e., extensive attachment with the jaw bone). The tooth crowns are pointed, recurved, and probably compressed mediolaterally, but it is difficult to assess how strong the compression is. No groove or ridge (cutting edges) is discernible along the anterior or posterior tooth margins. The teeth are well spaced, small anteriorly and becoming larger posteriorly. Many replacement teeth are preserved, and represent at least two generations. The tooth number is uncertain, but the estimated maximum of 10 maxillary teeth is based on the distribution of the preserved teeth on both the left and right maxilla, whereas tooth counts for premaxillary and dentary are estimated at about eight and 11 respectively. The palatal teeth are arranged in roughly two rows on the pterygoid and are present on palatine, again possibly in two rows (Figure S4B). They are small simple bulging structures. Palatal teeth are absent in *Varanus* and *Heloderma*, but are present in *Lanthanotus* (single row on pterygoid, variably on palatine, McDowell & Bogert, 1954), *Ovoo* (single palatine row, two pterygoid rows, Norell, Gao, & Conrad, 2007), and *Saniwa ensidens* (single continuous row on palatine and pterygoid, Gilmore 1928).

No hyoid elements were identified across the whole block.

Postcranial Skeleton

The elements of the postcranial skeleton (Figure 1) are disarticulated, but most of them are massed together in a small area of the block and clearly belong to a single individual.

Vertebral column. The specimen preserves 20 procoelous presacrals (including the axis and at least two further cervicals), two sacrals, 11 disarticulated caudals, and a further series of articulated caudals. Accurate counts of the cervical, trunk and caudal vertebrae are not possible. The presacral count in *Varanus* ranges from 27 to 35, with most species having 28-29 (Cieri, 2018), and there are 31 presacrals in *Saniwa ensidens* (Rieppel & Grande, 2007), 34 in *Heloderma*, and 36 in *Lanthanotus* (McDowell & Bogert, 1954).

The elements of the atlas have not been identified, but the axis (Figures 1B, S8F) lies beside the left femur and is almost complete. It is exposed in right lateral view, but the right prezygapophysis and the right half of the condyle are missing. The neural spine is anteroposteriorly expanded, and a hypapophysis (and the corresponding intercentrum) is present. The neural spine extends slightly beyond the posterior termination of the condyle but does not reach that of the hypapophyses. The synapophysis is broken and therefore its orientation is unknown. A second intercentrum appears to be present *in situ,* partially fused with the axis. There are another two cervical vertebrae preserved (judging by the presence of hypapophyses), one near the skull (Figure S2), and the other above the tibia (Figures S2, S8G). The former is preserved in left lateral view with the neural spine broken away, and the second seems to be associated with a separated epiphysis. It is difficult to tell whether the distal tips of the hypapophyses widen laterally but they are clearly enlarged, as evidenced by the one above the left tibia.

The trunk (dorsal) vertebrae are mostly exposed in ventral view, showing a clear precondylar constriction (Figures 1B, S8E). Some other vertebrae, preserved in lateral or dorsal view, show a complete or nearly complete neural spine. Where preserved, the synapophyses are massive, dorsoventrally elongated, and located just below the prezygapophysial process (Figure S8B). The vertebral condyle is compressed and faces dorsally and posteriorly, and the neural spine bears a horizontal dorsal margin that is slightly thickened posteriorly (Figures S8A, S8B), as in *Varanus*, *Lanthanotus* (Rieppel, 1980) and *Saniwa ensidens*. The anterior margin of the neural spine varies in its orientation along the presacral series from posterodorsally inclined to vertical (Figure 1B), and neural spine height probably also varied. Striations are evident on the neural arch (Figure S8A) (fibrous striae in Georgalis, Abdel Gawad, Hassan, El-Barkooky, & Hamdan, 2020). Smith et al. (2008) suggested that vertebral striae might have arisen on the *Varanus* stem and have been retained as a plesiomorphy in many crown *Varanus*, especially the African species. These striae are also obvious on the trunk vertebrae of *Saniwa ensidens* supporting the suggestion of Smith et al. (2008) that this feature was already present by the Eocene.

One trunk vertebra (Figure S2, trV-a), lying adjacent to the right lower jaw, has a neural spine only slightly longer than tall (i.e., it is an anterior trunk vertebra) and the anterior margin of the spine is posterodorsally inclined. On the two trunk vertebrae which were removed from the main postcranial mass, the neural spines are rectangular in shape with a vertical anterior margin and are much longer than tall (ratio is about 2:1), suggesting they are middle or middle-posterior trunk vertebrae (Figure S8B). Accessory articulations are present between successive neural arches (Figures S8C, S8D), and correspond to Hoffstetter's (1969) definition of a pseudozygosphene in having an anterior lamina that underlaps the posterior margin of the neural arch of the preceding vertebra (Hoffstetter, 1969). The pseudozygantrum, if treated as an accessory articulation, is evidently present in IVPP V 22770. Rieppel and Grande (2007) followed Hoffstetter (1969) and regarded a pseudozygosphene as present variably in *Saniwa endensis*, but it might be non-articular as a pseudozygantrum is absent. A pseudozygosphene is also present in some *Varanus*, but seems to be a non-homologous structure on the anterior margin of the neural arch (Conrad et al., 2012). Hoffstetter (1969) suggested that the pseudozygosphene is for the attachment of intervertebral muscles, but the presence of both pseudozygosphene and pseudozygantrum in *Archaeovaranus* vertebra argues against this hypothesis. Therefore, the presence or absence of the pseudozygosphene should be treated with caution when comparing different species from the literature.

Both sacral vertebrae (Figure S8H) are preserved in ventral view and are in articulation. Their centra are shorter than those of the presacrals. The transverse processes of the first sacral are robust and that of the second is slender (left side only complete).

Two caudal vertebrae (Figure 1B) are preserved near the sacrals and, based on their morphology, they are probably anterior caudals but not pygals as pedicels for haemapophyses are present on both, placed just anteroventral to the condylar articulation. The pleurapophyses are preserved but are not complete on either side. Several disarticulated caudals with tall neural spines and haemal arch pedicles (e.g., those in Figures S8G, S8I) are scattered on the block, from close to the skull to the

middle of the postcranial mass. The posterior tail is linear with the vertebrae in articulation (Figure 1B, tail; Figure S8J). There are no autotomy fracture planes visible in any preserved caudals.

The ribs are not associated with the vertebrae and show a generally similar morphology with an anteroposteriorly elongated articular head.

Pectoral girdle and Forelimbs. The left scapula and coracoid are exposed in lateral view (Figures 1B, S9A). The two bones are detached from each other, but are in roughly anatomical positions. The scapula and the coracoid contribute equally to the glenoid. Based on the position of the supracoracoid foramen, there is a single coracoid emargination, and the plate-like shape of the bone ventral (anatomically) to this emargination is similar to that in *Saniwa ensidens* (Gilmore, 1928). This morphology distinguishes these taxa from both *Varanus* and *Lanthanotus* (Rieppel, 1980) where there are two coracoid emarginations, and from *Heloderma* where there are none. The spike-like process remaining above the coracoid emargination sutures to the scapula and contributes to the border of the scapulocoracoid emargination. As preserved, the scapula is broad and, as in *Varanus* and *Lanthanotus*, there seems to be no scapular emargination.

Both humeri (Figures 1B, S9B) are preserved. They are robustly built and show little torsion. The left humerus is completely exposed in dorsal view, but only the proximal half of the right bone is visible. The proximal epiphysis is ossified and completely fused with the humerus, but the distal epicondylar epiphyses are missing on both sides. Both ends of the humerus are greatly expanded. The proximal humeral condyle, medial tuberosity, and lateral tuberosity are distinct. A deltopectoral crest is present, but its size is difficult to assess. The distal end of the bone bears a broken posterior (anatomical) margin that suggests the presence of an ectepicondylar foramen. Overall, the configuration of the humerus is similar to that of *Varanus* (for example *V. salvator*), and more robust than that of *Lanthanotus* (Rieppel, 1980).

Neither radius is preserved. The right ulna (preserved with the skull mass) (Figure 1A, ul; Figure S9C) bears a prominent olecranon process, and a deep posterior fossa like that in some *Varanus*.

Pelvis and hind limb. No pelvic elements have been identified.
Both femora are preserved (Figures 1B, S9D), and are similar in length to the humeri (removing the distal epicondyles of both). The right femur is complete in dorsal view and the left one is exposed only at the distal end. The proximal femoral condylar epiphysis is present and fused with the shaft, but the internal trochanter is buried in the matrix. The distal epicondyle is missing, suggesting that it had not fused with the femoral shaft.

Both tibiae and fibulae are preserved (Figures 1B, S9E, S9F). The proximal part of the right tibia and the distal part of the left one are located posterior to the right femur. Both the fibulae are preserved without epiphyses. Further details are difficult to discern.

As preserved, the right astragalus is separate from the calcaneus, as in *Saniwa ensidens* (FMNH PR 2378). The fusion of the astragalus and calcaneus occurs very

late during development in at least some *Varanus* (see discussion below on the ontogenetic stage of IVPP V 22770). The astragalus (Figures 1B, S9G) is compressed and plate-like, exposing the tibial facet and half of the fibular facet. The two facets are separated by a prominent notch as in *Varanus*. The distal margin, although incomplete, displays a concavity for articulation with the fourth distal tarsal. The antero-distal border of the bone is slightly thickened as in *Varanus*.

Some metacarpals / metatarsals and phalanges (Figures 1B, S9H) are preserved *in situ* and partially articulated, but their detailed morphology is difficult to determine.

Discussion

The phylogenetic position of *Archaeovaranus lii*

As outlined in the Material and Methods section (and also in more detail in the supplementary Text S3), two analyses were run using the data matrix of Gauthier et al. (2012), with or without a molecular constraint, and then eight different phylogenetic analyses were run using the matrix of Villa et al. (2018), with different outgroup taxa (*Shinisaurus* or *Heloderma*) and with a subset of marine dolichosaurs included or excluded. Using the Gauthier et al. (2012) matrix, the first (unconstrained) analysis found 12 MPTs with a tree length of 5326 steps while the second (constrained) analysis produced 1680 MPTs with a length of 5481 steps. Both analyses recovered *Archaeovaranus lii* within Anguimorpha. The strict consensus tree of the unconstrained analysis positioned *Archaeovaranus lii*, together with *Aiolosaurus oriens* (Late Cretaceous, Gobi Desert), on the stem of a clade comprising *Lanthanotus*, *Saniwa* and *Varanus* (Figure S11), whereas the strict consensus of the constrained analysis placed *Archaeovaranus lii* as the sister taxon of *Varanus* (Figure S12).

Using the Villa et al. (2018) matrix, the choice of the outgroup did not affect the tree length, MPTs, or the topology of the strict consensus trees (Figures S13-S24). Whether dolichosaurs are included or not does not influence the ingroup relationships of the genus *Varanus* in the combined analyses but their inclusion did affect the placement of *Paranecrosaurus* and *Eosaniwa* in the morphology only analyses. Moreover, the placement of dolichoaurs themselves also differed between the analyses depending on whether combined evidence or morphological characters alone were used. This reflects the lack of consensus between other researchers (e.g. Conrad et al., 2011; Gauthier et al., 2012; Reeder et al., 2015; Simões et al., 2017). Nonetheless, the positions of the other taxa were relatively stable across all the analyses. The combined analyses recovered some of the known clades within *Varanus*, such as the *gouldii* group (part of the *Varanus* subgenus) and the *Odatria* subgenus of the Indo-Australian clade, and the two Indo-Asian clades, but the other *Varanus* species collapsed probably due to poorly preserved fossil taxa such as *Varanus cf. bengalensis*.

Saniwa ensidens had long been regarded as the closest relative of *Varanus* based on morphological comparison (e.g., Gilmore, 1928) (McDowell & Bogert, 1954), morphological character analysis (e.g. Lee, 1997) (Conrad, Grande, & Rieppel, 2008), and combined analyses with an extensive molecular data set (e.g. Villa et al., 2018) (Brennan et al., 2021). However, each of the analyses using the matrix of Villa et al. (2018) and the constrained analysis of the Gauthier et al. (2012) matrix herein, all placed *Archaeovaranus* as the sister taxon of *Varanus*, with *Saniwa ensidens* as the

sister taxon to these two. Figure 3 shows the strict consensus (136 MPTs, Tree length 10700, CI 0.311, RI 0.451) of an analysis using the Villa et al. (2018) combined evidence matrix, with *Heloderma* as the designated outgroup, and dolichosaur taxa de-activated.

Stem-ward of the *Saniwa*+(*Archaeovaranus*+*Varanus*) clade there is a succession of varaniforms from the Late Cretaceous of Mongolia including *Telmasaurus grangeri* (Gilmore, 1943), *Saniwides mongoliensis* (Borsuk-Białynicka, 1984), *Aiolosaurus oriens* (Gao & Norell, 2000), and *Ovoo gurvel* (Norell, Gao, & Conrad, 2007), with the lanthanotids (*Lanthanotus* and the Late Cretaceous Mongolian *Cherminotus*) as sister to those (Figures 3, S13-S24). The European Paleogene palaeovaranids (sensu Georgalis, 2017) *Ophisauriscus* (‘*Necrosaurus*’) *eucarinatus* and *Paleovaranus* (‘*Necrosaurus*’) *cayluxi* were positioned on the stem of the *Lanthanotus* + *Varanus* clade, but not as sister taxa, and the positions of *Paranecrosaurus (‘Saniwa’) feisti* (Smith & Habersetzer, 2021) and *Eosaniwa kuhni* clade varied depending on the inclusion or exclusion of dolichosaurs, and the use of morphological or combined evidence. This contrasts with the findings of Smith and Habersetzer (2021) who found a palaeovaranid clade as the sister group of Lanthanotidae+Varanidae.

Comparison with other fossil and extant varanid relatives

Although phylogenetic analyses using morphological characters usually place *Heloderma* and its fossil relatives as the sister group of *Varanus*+*Lanthanotus* (e.g. Estes et al., 1988; Gauthier et al., 2012), analyses incorporating molecular data generally place *Heloderma* closer to anguids (e.g. Vidal et al., 2012; Pyron et al., 2013; Reeder et al., 2015; Burbrink et al., 2020) than to varanids (i.e. they are not varaniforms). This means that several characters occurring in both Varanidae and Helodermatidae (e.g. plicidentine, a short maxilla, well-spaced recurved teeth, an elongated anterior coronoid process, narrow vomers, cristae cranii of the frontals meeting in the midline under the olfactory tracts, and a posteriorly extended external narial opening) arose at least twice, likely due to the predatory habits of these lizards (Smith & Habersetzer, 2021). These common characters complicate comparisons with fossil taxa, especially when the representative specimens are incomplete. Nonetheless, *Heloderma* differs from both *Varanus* and *Lanthanotus* in having a single lacrimal foramen and paired nasals (contra two lacrimal foramina and fused nasals), in having thick tubercular osteoderms, and in lacking a palpebral and an intramandibular joint.

Designated palaeovaranids (sensu Georgalis, 2017; Smith & Habersetzer, 2021) including *Ophisauriscus*, *Palaeovaranus*, and *Paranecrosaurus* differ from lanthanotids and total group varanids in having a single lacrimal foramen, a more limited external narial extension, and in lacking a functional intramandibular joint (Smith & Habersetzer, 2021). However, in our analysis, these taxa did not form a monophyletic group.

Total group Varanidae (stem+crown) differs from known lanthanotids in several characters including longer and narrower nasals and an elongated anterior process of the coronoid that clasps the dentary. Other characters like nasal fusion (*Aiolosaurus oriens,* Gao & Norell 2000; some *Varanus*, Mertens, 1942), the presence of plicidentine (unknown in *Aiolosaurus*), the position of the dorsal lacrimal foramen (within lacrimal or at prefrontal-frontal margin) are unevenly distributed within this stem-varanid group. This distribution could reflect instability in this part of the tree,

but also that these characters are labile, as evidenced by the morphology of *Heloderma*.

Archaeovaranus lii and *Saniwa ensidens* differ from the Late Cretaceous stem-varanids and resemble *Varanus* in the posterior extension of the external narial openings to reach the frontals, the fusion of the nasals into a narrow midline bar, and the presence of an intramandibular joint. The skull roof in *Archaeovaranus* looks similar to that in *Saniwa ensidens* (i.e. extended external narial openings, unpaired nasal, paired frontals), except that the snout is longer and the frontal is relatively shorter in *Archaeovaranus*. In the palate, there are two continuous rows of teeth on palatine and pterygoid in *Archaeovaranus*, but only one row in *Saniwa* (Gilmore, 1928). There are two internal hypoglossal foramina in *Archaeovaranus*, but only one in *Saniwa* (Rieppel & Grande, 2007) and *Lanthanotus*. The condition in *Varanus*, however, may be variable with one or two internal foramina (Evans, 2008).

Archaeovaranus resembles *Varanus*, and differs from *Saniwa* in several features that support its sister group relationships (see supplementary Text S4). These include having a slightly shorter maxillary tooth row (one tooth extends below the orbit in *Archaeovaranus* vs two to three in *Saniwa*) and a premaxilla with a posteriorly tapering nasal process (the tip of the process in *Saniwa* is slightly expanded and bifurcated rather than tapered (Rieppel & Grande, 2007)). A small parietal tab is present on the frontal in *Archaeovaranus*, resembling the condition in *Varanus*, but not *Saniwa* (Rieppel & Grande, 2007). As in *Varanus*, the dorsal lacrimal foramen of *Archaeovaranus* is enclosed by the prefrontal and the lacrimal whereas both lacrimal foramina are fully enclosed by the lacrimal in *Saniwa* (Rieppel & Grande, 2007).

Despite the similarities, *Archaeovaranus* differs from *Varanus* in several characters, where it shows the primitive state. In *Archaeovaranus* the cristae cranii of the frontals are completely separate from each other whereas they meet or nearly meet in the midline in *Varanus*; the bony postorbital bar is completed by the jugal in *Archaeovaranus* but it is incomplete due to the loss of the jugal-postorbital articulation in *Varanus*; there are both palatine and pterygoid teeth in *Archaeovaranus*, but none in *Varanus*. The otooccipital in *Archaeovaranus* has a deep notch lateral to the vagus foramen in occipital view, but the notch is absent or very shallow in *Varanus*. The basisphenoid-basioccipital suture in *Archaeovaranus* is inverted V-shaped with a flat vertex, but transverse in *Varanus*. In *Archaeovaranus*, the scapula is unemarginated, there is a scapulocoracoid emargination, and the coracoid has a single emargination, but in *Varanus* and *Lanthanotus* the coracoid has two emarginations.

The size and ecology of *Archaeovaranus lii*

To estimate the total length of the long bones in *Archaeovaranus* holotype (IVPP V 22770), we measured the length of these bones with and without epiphyses in the specimen (supplementary Table S4) and *Varanus* specimens from the NHM London (Table S5-S8). We then ran regressions of these to calculate an estimated total femur length (i.e. including the epiphyses) of 43.48 mm for the holotype specimen of *Archaeovaranus*, and a total humerus length of 43.04 mm. The estimated total ulna and fibula lengths were 29.84 mm and 31.94 mm respectively. However, note that the estimate of total ulna length for the *Archaeovaranus lii* holotype, as calculated using the regression of the NHM dataset, was less (at 29.84 mm) than the actual measured

length of the ulna as preserved (31.47 mm), with the proximal (olecranon) but not distal epiphysis. For this reason, the actual measured length of the ulna was used in the calculations of total limb length. This represents a slight underestimate of the ulna length in life, but as the distal ulna epiphysis in *Varanus* is less than half the size of the proximal epiphysis, the difference is quite small. We then used several different datasets to estimate the snout to vent length (SVL) and the total length (TL) of IVPP V 22770. The SVL estimates ranged from 313.23 to 512. 49 mm, with a total length estimate from 802.79 to 1254.87 mm (Table S9) based on a regression analysis from the combined data (Data S2) of Conrad et al. (2012) and Schuett, Reiserer, & Earley (2009).

Although the body form of Varanidae has been described as conservative (Pianka, 1995), the extant species of *Varanus* are ecologically diverse (terrestrial, saxicolous, semiaquatic, and arboreal), and a study of *Varanus* showed that its species converged repeatedly on body plans and ecological niches (Brennan et al., 2021).

Thompson and Withers (1997) analyzing the relative limb dimensions of 17 Australian *Varanus*, suggested that they are morphologically diverse. They found a link between semi-aquatic habits and limb proportions, although the results were not conclusive (Thompson & Withers, 1997). Thompson et al. (2008) later suggested a strong link between the body shape, as represented by morphometric characters such as body length and forelimb length, and the retreat preferences of *Varanus* spp. in Western Australia, and concluded that the morphometric disparity might be a combined effect of phylogeny, sex, and ecology with body size also an important factor (Thompson, Clemente, Withers, Fry, & Norman, 2008).

In *Archaeovaranus* the forelimb (humerus + ulna) and hind limb (femur + fibula) are of similar length (FL/HL proportion is 0.988), as are the humerus and femur (H/F proportion is 0.990). These proportions are not only outside the normal range of *Varanus* spp. (usually well below 1) but are also rare among limbed squamates generally (Villaseñor-Amador, Suárez, & Alberto Cruz, 2021), although these authors were unable to link these limb proportions to any particular lifestyle. The other Eocene stem-varanid *Saniwa ensidens* resembles *Archaeovaranus* in being of medium-size as (Conrad et al., 2012), but has different proportions of the forelimb in relation to the hind limb (0.912) and of the humerus/femur (0.853). This species was firstly interpreted as terrestrial based on its possession of a tail that is rounded rather than bilaterally compressed with tall neural spines, as might be expected in a swimmer (Gilmore, 1922). In contrast, Rieppel and Grande (2007) suggested the unfused astragalus and calcaneum in FMNH PR2378 could possibly indicate that *Saniwa* was semiaquatic. These same authors also reported that body proportions placed *Saniwa ensidens* FMNH PR 2378 between the arboreal *Varanus prasinus* and the semi-aquatic *Varanus salvator*. However, although the data for *Saniwa ensidens* remains inconclusive, the relatively longer forelimb in *Archaeovaranus* suggests the two species may have had different lifestyles.

Bone histology of *Archaeovaranus lii*, and the ontogenetic stage of the holotype

The timing of closure of the astragalocalcaneal suture in the ankle is variable among squamates, and an open suture may therefore be an age-dependent factor (Russell & Bauer, 2008). Our observation of the rib histology of the extant *Varanus salvator* shows an obvious decrease in growth rate near the periosteal surface (a broader layer

of parallel-fibered bone indicated by the outer blueish region in Figure S10B) in an individual with a clear astragalocalcaneal suture, and indicates that the fusion between astragalus and calcaneum occurs late in *Varanus*, as Rieppel and Grande (2007) argued.

The validity of growth marks in different bone elements of *Varanus* has been discussed by previous researchers (de Buffrénil & Castanet, 2000). The fibula usually retains more Skeletal Growth Marks (SGMs) than the femur, tibia or phalanges in large individuals of *Varanus* (de Buffrénil & Castanet, 2000), because the fibula bears less weight than other hind limb bones and has less medullary resorption. We therefore chose the fibula in our study for age estimation, with the caveat that the fibula may appear to be older than other bone elements in a single skeleton (Zhao et al. 2019).

Although a thin section of the right fibula (Figure S10A) indicated that its tissue had been partly modified by diagenesis, the principal bone tissue can still be recognised as parallel-fibered bone. The vascularization is very poor with no osteons present in the cortex, a condition similar to that in *Sphenodon punctatus* (Scheyer et al. 2010). Most of the osteocyte lacunae are oval or nearly round with numerous canaliculi. Bone remodelling is very rare in the cortex, and no secondary osteons or endosteal bone were observed. Two types of SGMs, lines of arrested growth (LAGs) and annuli, were recognized and were used for the age estimation. The first SGM, which was defined as the "neonatal line" by previous authors (de Buffrénil & Castanet, 2000), is about 36 μm in diameter, and most of it has been resorbed by the medullary cavity. The second and third SGMs can be recognized as LAGs, because they are more birefringent than annuli under transmitted polarized light. The fourth to sixteenth SGMs are annuli with parallel-fibered tissue, and between these annuli are woven fibered primary periosteal tissue. A total of 16 SGMs are present in the cortex in IVPP V 22770, giving an age estimate of 16 years old for this individual. The spacing between the adjacent SGMs decreased dramatically after the fifth SGM, indicating that the growth rate dropped and reproductive maturity may have occurred at this age. The narrowing of intervals between the outer SGMs with no typical EFS (external fundamental system, Cormack, 1987), indicates that this individual was still growing but at a very slow rate.

The evolution of varanid cranial characters

The skull of extant species of *Varanus* is characterized by many distinctive features, including an elongated snout, posteriorly extended ('retracted') external narial openings nares, median narial bar, cristae cranii that meet or nearly meet below the frontal, loss of a complete postorbital bar, and development of an intramandibular joint. *Lanthanotus, Archaeovaranus,* and *Saniwa* share the enlarged external narial openings and fused nasals, but differ from *Varanus* in having a complete postorbital bar and cristae cranii that do not meet in the midline (Figure 3A). Thus the midline contact of the cristae cranii to create a strong cylindrical frontal seems to coincide with the loss of the bony postorbital bar in the evolution of *Varanus* itself.

The South American teiid lizard *Salvator merrianae* is of similar size and lifestyle to *Varanus niloticus*, and the two species have a comparable bite force (Dutel et al., 2021). However, the skull of *Salvator* differs from that of *Varanus* in snout structure, and in having a complete postorbital bar and weakly developed cristae cranii on the

frontal. Dutel et al. (2021) found that the postorbital bar of *Salvator* experienced very high strain magnitudes during biting, especially in bites by the posterior teeth, and that removal of the bar significantly increased strain magnitudes in other parts of the skull. The postorbital bar is therefore important in maintaining skull integrity during biting in *Salvator*. Artificially modeling a postorbital bar on to *Varanus* decreased strain magnitudes across the skull to some degree, whereas removing the ventrally united cristae cranii (subolfactory processes) in the *Varanus* model significantly increased strain levels, particularly in the frontal. Extension and fusion of the cristae cranii in *Varanus* therefore strengthen the interorbital region of the skull, permitting loss of the postorbital bar without compromising skull rigidity (Dutel et al. 2021). The interorbital region experiences high levels of strain in *Varanus* during feeding movements like prey shaking and pull-back cutting that draws teeth through prey items (McCurry et al., 2015). A similar combination of cylindrical frontal and loss of the postorbital bar is seen in gekkotan lizards, where loss of the postorbital bar has been linked to increasing eye size and mesokinetic (fronto-parietal) cranial kinesis (Herrel et al., 2000). The advantage to *Varanus* of losing the postorbital bar is less obvious as the eyes are not unusually large, and many varanids – especially the larger species – seem to have little or no kinesis (Herrel et al., 2007). However, loss of the bar may originally have been associated with mesokinesis, with subsequent loss or reduction of kinesis in some species, or it may have been secondary to strengthening the frontal, thereby helping to lighten the skull for fast inertial feeding, and create additional space for adductor muscles.

Saniwa and *Archaeovaranus* thus represent a stage of varanid evolution in which the long, fenestrated and flattened snout had already evolved, potentially increasing their ability to catch fast-moving prey (Metzger & Herrel, 2005), but without the strengthening of the frontal region and subsequent loss of the postorbital bar (Figure 3A). In *Varanus*, the reduction of the tongue for a primarily sensory role, means that it can no longer be used for prey transport in the mouth and *Varanus* therefore uses inertial feeding (Herrel et al. 2007). However, the retention of palatal teeth in *Saniwa* and *Archaeovaranus* (lost in *Varanus*) is indicative of an interaction between the tongue and the palate in transferring prey toward the back of the mouth, suggesting the tongue of the extinct genera may have been fleshier, permitting lingual transport rather than inertial feeding. Unfortunately, very little information is available about the feeding behavior of *Lanthanotus*, which also retains palatal teeth. The tongue is said to be divided into a thin, bifurcate anterior part (McDowell & Bogert, 1954) used, as in *Varanus*, for chemosensation, and a thicker posterior part. However, *Lanthanotus* has been observed to feed underwater, swallowing objects whole, but not surfacing to use inertial feeding (Mendyk, Shuter & Kalkriner, 2015). *Shinisaurus*, the extant sister taxon to *Lanthanotus* and *Varanus* (Conrad, 2008), also has palatal (pterygoid) teeth and has been observed to use the tongue for intraoral transport, but not inertial feeding (Tchobanov, 2015).

The origin and palaeobiogeography of varanids

The divergence between lineages leading to *Varanus* and *Lanthanotus* has been dated to the mid-Cretaceous, around 80-100 Ma (Brennan et al., 2021), and a recent estimate places the crown age of *Varanus* as early to middle Oligocene (Lin & Wiens, 2017) (Brennan et al., 2021). However, the earliest definitive *Varanus* remains are from the early Miocene (Clos, 1995) (Ivanov et al., 2017) (Figure 3A).

Several varaniform taxa (e.g. *Ovoo*, *Telmasaurus*, *Aiolosaurus, Saniwides, Proplatynota*) have been recorded from the Late Cretaceous deposits of the Gobi Desert (Gilmore, 1943; Borsuk-Białynicka, 1984; Gao & Norell, 2000; Norell, Gao & Conrad, 2007), but their precise relationships to *Varanus* and *Lanthanotus* vary between published phylogenetic trees (e.g. Conrad et al., 2008; Norell, Gao & Conrad, 2007; Brennan et al., 2021; Smith & Habersetzer, 2021). In our analysis, all these taxa except *Cherminotus* were placed on the varanid stem. A second varaniform group has been described from the Palaeogene of Europe (Palaeovaranidae sensi Georgalis, 2017, Smith & Habersetzer, 2021), but their proposed placement varies (sister to Lanthanotidae, Brennan et al., 2021; or to Varanidae + Lanthanotidae, Smith & Habersetzer, 2021), and our analyses did not recover it as a monophyletic group. The only Paleogene taxon that had consistently been placed as a sister taxon to *Varanus* was *Saniwa ensidens* from the Eocene of North America (Gilmore, 1928) (Rieppel & Grande, 2007), although vertebrae referred to *Saniwa* or stem *Varanus* have been reported from the earliest Eocene, or earlier middle Paleocene to late Oligocene across North America, Europe, Africa, and Asia (Augé, 1990) (Dong et al., 2016) (Smith, 2009) (Smith et al., 2008; Holmes et al., 2010) (Zerova & Chkhikvadze, 1986) (Averianov & Danilov, 1997).

Both molecular and morphological data support an Asian origin for Varanidae (Estes, 1983) (Vidal et al., 2012) (Conrad et al., 2012) (Brennan et al., 2021), although some researchers have presented molecular or paleontological support for an African or Gondwanan origin (Holmes et al., 2010) (Schulte, Melville, & Larson, 2003). A recent analysis (Brennan et al. 2021) also placed the origin of varaniform lizards in East Asia with subsequent dispersal to Europe, and North America, and the origin of *Varanus* was proposed to have followed a similar pattern. The discovery of *Archaeovaranus lii* from the early Eocene in central China suggests that the transition from Cretaceous varaniform lizards to *Varanus* could have occurred in East Asia before the origin and dispersal of *Varanus* to other regions took place. *Archaeovaranus* therefore fills a significant gap in the fossil record of varanids by clearly demonstrating the presence of a stem-varanid closely related to *Varanus* in the early Eocene of East Asia.

References

Alifanov, V. 1993. Some peculiarities of the Cretaceous and Palaeogene lizard faunas of the Mongolian People's Republic. *Kaupia – Darmstädter Beiträge zur Naturgeschichte*, 3, 9-13.

Augé, M. (1990). *La faune de lezards et d'amphisbaenes (Reptilia, Squamata) du gisement de Dormaal (Belgique, Eocene inferieur)* (60). Bruxelles, Belgique: Institut Royal des Sciences naturelles de Belgique.

Auliya, M. & Koch, A. (2020). Visual identification guide to the Monitor lizard species of the world (genus *Varanus*). *Bundesamt für Naturschutz*, BfN-Skripten 552.

Averianov, A. O., & Danilov, I. G. (1997). A varanid lizard (Squamata: Varanidae) from the Early Eocene of Kirghizia. *Russian Journal of Herpetology*, 4(2), 143-147.

Bellairs, A. (1949). Observations on the snout of *Varanus*, and a comparison with that of other lizards and snakes. *Journal of Anatomy*, 83(Pt 2), 116.

Böhme, W. (2003). Checklist of the living monitor lizards of the world (family Varanidae). *Zoologische Verhandelingen*, 341, 4-43.

Borsuk-Białynicka, M. (1984). Anguimorphans and related lizards from the Late Cretaceous of the Gobi Desert, Mongolia. *Palaeontologia Polonica*, 46, 5-105.

Brennan, I. G., Lemmon, A. R., Lemmon, E. M., Portik, D. M., Weijola, V., Welton, L. et al. (2021). Phylogenomics of monitor lizards and the role of competition in dictating body size disparity. *Systematic Biology*, 70, 120-132.

Burbrink, F. T., Grazziotin, F. G., Pyron, R. A., *et al*. (2020). Interrogating genomic-scale data for Squamata (lizards, snakes, and amphisbaenians) shows no support for key traditional morphological relationships. *Systematic Biology*, 69(3), 502–520.

Chen, Z., Ding, Z., Yang, S., & Zhang, C., Wang, X. (2016). Increased precipitation and weathering across the Paleocene-Eocene Thermal Maximum in central China. *Geochemistry*, *Geophysics, Geosystems* 17 (6), 2286-2297.

Chen, Z., Wang, X., Hu, J., Yang, S., Zhu, M., Dong, X. et al. (2014). Structure of the carbon isotope excursion in a high-resolution lacustrine Paleocene–Eocene Thermal Maximum record from central China. *Earth and Planetary Science Letters*, 408, 331-340.

Cieri, R. L. (2018). The axial anatomy of monitor lizards (Varanidae). *Journal of Anatomy*, 233(5), 636-643.

Clos, L. M. (1995). A new species of *Varanus* (Reptilia: Sauria) from the Miocene of Kenya. *Journal of Vertebrate Paleontology*, 15(2), 254-267.

Conrad, J. L. (2008). Phylogeny and systematics of Squamata (Reptilia) based on morphology. *Bulletin of the American Museum of Natural History*, Number 310, 1-182.

Conrad JL, Ast JC, Montanari S, & Norell MA. (2011). A combined evidence phylogenetic analysis of Anguimorpha (Reptilia: Squamata). *Cladistics*, 27, 230-77

Conrad, J. L., Grande, L., & Rieppel, O. (2008). Re-assessment of varanid evolution based on new data from *Saniwa ensidens* Leidy, 1870 (Squamata, Reptilia). *American Museum Novitates*, 3630, 1-16.

Conrad, J. L., Balcarcel, A. M., & Mehling, C. M. (2012). Earliest example of a giant monitor lizard (*Varanus*, Varanidae, Squamata). *PloS One*, 7(8), e41767.

Cormack D. (1987). *Ham's Histology***.** Lippincott, New York. 732 p.

de Buffrénil, V., & Castanet, J. (2000). Age estimation by skeletochronology in the Nile monitor (*Varanus niloticus*), a highly exploited species. *Journal of Herpetology*, 34, 414-424.

de Buffrénil, V., Ineich, I., & Böhme, W. (2004). Comparative data on epiphyseal development in the family Varanidae. *Journal of Herpetology*, 37(3), 328-335.

Dong, L., Evans, S. E., & Wang, Y. (2016). Taxonomic revision of lizards from the Paleocene deposits of the Qianshan Basin, Anhui, China. *Vertebrata PalAsiatica*, 54(3), 243-268.

Dutel, H., Gröning, F., Sharp, A. C., Watson, P. J., Herrel, A., Ross, C. F. et al. (2021). Comparative cranial biomechanics in two lizard species: impact of variation in cranial design. *Journal of Experimental Biology*, 224(5), jeb234831.

Estes, R. (1983). *Sauria Terrestria, Amphisbaenia. Encyclopedia of Paleoherpetology, Part 10A*. Gustav Fischer Verlag, Stuttgart, New York.

Estes, R., Queiroz, K. D., & Gauthier, J. (1988). Phylogenetic relationships within Squamata. In R. Estes & G. Pregill (Eds.), *Phylogenetic relationships of the lizard families—Essays Commemorating Charles L. Camp* (pp. 119-281). Stanford, California: Stanford University Press.

Evans, S. E. (2008). The skull of lizards and Tuatara. In G. Gans, A. S. Gaunt, & K. Adler (Eds.), *The Skull of Lepidosauria* (Vol. 20, Morphology H, pp. 1-344). New York: Ithaca.

Gao, K., & Norell, M. A. (2000). Taxonomic composition and systematics of Late Cretaceous lizard assemblages from Ukhaa Tolgod and adjacent localities, Mongolian Gobi Desert. *Bulletin of the American Museum of Natural History*, Number 249, 1-118.

Gauthier, J. A., Kearney, M., Maisano, J. A., Rieppel, O., & Behlke, A. D. B. (2012). Assembling the squamate tree of life: perspectives from the phenotype and the fossil record. *Bulletin of the Peabody Museum of Natural History*, 53(1), 3-308.

Georgalis, G. L. (2017). *Necrosaurus* or *Palaeovaranus*? Appropriate nomenclature and taxonomic content of an enigmatic fossil lizard clade (Squamata). *Annales de Paléontologie*, 103, 293-303

Georgalis, G. L., Abdel Gawad, M. K., Hassan, S. M., El-Barkooky, A. N., & Hamdan, M. A. (2020). Oldest co-occurrence of *Varanus* and *Python* from Africa—first record of squamates from the early Miocene of Moghra Formation, Western Desert, Egypt. *Peer J*, 8, e9092.

Gilmore, C. W. (1922). A new description of *Saniwa ensidens* Leidy, an extinct varanid lizard from Wyoming. *Proceedings of the US National Museum*, 60 (23), 1-31.

Gilmore, C. W. (1928). *Fossil Lizards of North America*. Riverside Museum Press.

Gilmore, C. W. (1943). Fossil lizards of Mongolia. *Bulletin of the American Museum of Natural History*, 81(4), 361-384.

Goloboff, P. A., & Catalano, S. A. (2016). TNT version 1.5, including a full implementation of phylogenetic morphometrics. *Cladistics*, 32(3), 221-238.

Head, J. J., Barrett, P. M., & Rayfield, E. J. (2009). Neurocranial osteology and systematic relationships of *Varanus* (*Megalania*) *prisca* Owen, 1859 (Squamata: Varanidae). *Zoological Journal of the Linnean Society*, 155(2), 445-457.

Herrel, A., Aerts, P., & De Vree F. (2000). Cranial kinesis in geckoes: functional implications. *Journal of Experimental Biology*, 203, 1415-1423.

Herrel, A., Schaerlaeken, V., Meyers, J. J., Metzger, K. A., & Ross, C. F. (2007). The evolution of cranial design and performance in squamates: Consequences of

skull-bone reduction on feeding behavior. *Integrative and Comparative Biology*, 47(1), 107–117.

Hoffstetter, R. (1969). Presence de Varanidae (Reptilia, Sauria) dans le Miocene de Catalogne. Considerations sur l'histoire de la famille. *Bulletin du Muséum national d'Histoire naturelle*, 40(1968), 1051-1064.

Holmes, R. B., Murray, A. M., Attia, Y. S., Simons, E. L., & Chatrath, P. (2010). Oldest known *Varanus* (Squamata: Varanidae) from the Upper Eocene and Lower Oligocene of Egypt: support for an African origin of the genus. *Palaeontology*, 53(5), 1099-1110.

Ivanov, M., Ruta, M., Klembara, J., & Böhme, M. (2017). A new species of *Varanus* (Anguimorpha: Varanidae) from the early Miocene of the Czech Republic, and its relationships and palaeoecology. *Journal of Systematic Palaeontology*, 16(9), 767-797.

Jiang, H., N. Zhong, Y. Li, H. Xu, X. Ma, Y. Meng, and X. Mao (2014). Magnetostratigraphy and grain size record of the Xijiadian fluviolacustrine sediments in East China and its implied stepwise enhancement of the westerly circulation during the Eocene period. *Journal of Geophysical Research: Solid Earth*, 119, 7442–7457, doi:10.1002/2014JB011225

Lee, M. S. Y. (1997). The phylogeny of varanoid lizards and the affinities of snakes *Philosophical Transactions of the Royal Society, London*, B352, 53-91

Lin, L., & Wiens, J. J. (2017). Comparing macroecological patterns across continents: evolution of climatic niche breadth in varanid lizards. *Ecography*, 40(8), 960-970.

Ma, A., & Cheng, J. (1991). On biostratigraphical subdivision of Yuhuangding Formation in Liguanqian Basin of Eastern Qinling Region. *Scientia Geologica Sinica*, 1991(1), 21-29 (in Chinese).

McCurry, M. R., Mahony, M., Clausen, P. D., Quayle, M. R., Walmsley, C. W., Jessop, T. S. et al. (2015). The relationship between cranial structure, biomechanical performance and ecological diversity in varanoid lizards. *PloS One*, 10(6), e0130625.

McDowell, J. S. B., & Bogert, C. M. (1954). The systematic position of *Lanthanotus* and the affinities of the anguimorphan lizards. *Bulletin American Museum of Natural History*, 105(Article 1), 1-142.

Mendyk, R. W., Shuter, A., & Kalkriner, A. (2015). Historical notes on a living specimen of *Lanthanotus borneensis* (Squamata: Sauria: Lanthanotidae) maintained at the Bronx Zoo from 1968 to 1976. *Biawak*, 9, 44-49.

Mertens, R. (1942). Die Familie der Warane (Varanidae)--Teil 2, Der Schädel. *Abhandlungen der Senckenbergischen Naturforschenden Gesellschaft,* 465*, 117-234*.

Metzger, K. A. & Herrel, A. (2005). Correlations between lizard cranial shape and diet: a quantitative, phylogenetically informed analysis. *Biological Journal of the Linnean Society*, 86, 433–466.

Norell, M., & Gao, K. (1997). Braincase and phylogenetic relationships of *Estesia mongoliensis* from the Late Cretaceous of the Gobi Desert and the recognition of a new clade of lizards. *American Museum Novitates*, *no.* 3211, 1-25.

Norell, M. A., Gao, K.-Q., & Conrad, J. (2007). A new platynotan lizard (Diapsida: Squamata) from the Late Cretaceous Gobi Desert (Ömnögov), Mongolia. *American Museum Novitates*, 3605, 1-22.

Oelrich, T. M. (1956). The anatomy of the head of *Ctenosaura pectinata* (Iguanidae). *Miscellaneous publications, Museum of Zoology, University of Michigan*, No. 94, 122.

Pianka, E. R., King, D., & King, R. A. (2004). *Varanoid Lizards of the World*. Bloomington & Indianapolis: Indiana University Press.

Pianka, E. R. (1995). Evolution of body size: varanid lizards as a model system. *The American Naturalist*, 146(3), 398-414.

Pyron, R. A., Burbrink, F. T. & Wiens, J. J. (2013). A phylogeny and revised classification of Squamata, including 4161 species of lizards and snakes. *BMC Evolutionary Biology*, 13, Art.93.

Reeder, T. W., Townsend, T. M., Mulcahy, D. G., Noonan, B. P., Wood, P. L., Sites, J. W. & Wiens, John J. (2015). Integrated analyses resolve conflicts over squamate reptile phylogeny and reveal unexpected placements for fossil taxa. *PloS One*, 10(3), e0118199.

Rieppel, O. (1980). The postcranial skeleton of *Lanthanotus borneensis* (Reptilia, Lacertilia). *Amphibia-Reptilia*, 1, 95-112.

Rieppel, O. (1983). A comparison of the skull of *Lanthanotus borneensis* (Reptilia: Varanoidea) with the skull of primitive snakes. *Zeitschrift für Zoologische Systematik und Evolutionsforschung*, 21, 142-153.

Rieppel, O., Gauthier, J., & Maisano, J. (2008). Comparative morphology of the dermal palate in squamate reptiles, with comments on phylogenetic implications. *Zoological Journal of the Linnean Society*, 152, 131-152.

Rieppel, O., & Grande, L. (2007). The anatomy of the fossil varanid lizard *Saniwa ensidens* Leidy, 1870, based on a newly discovered complete skeleton. *Journal of Paleontology*, 81(4), 643-665.

Russell, A. P., & Bauer, A. M. (2008). The appendicular locomotor apparatus of *Sphenodon* and normal-limbed squamates. In C. Gans, A. S. Gaunt, & A. Kraig (Eds.), *The Skull and Appendicular Locomotor Apparatus of Lepidosauria* (Vol. 21, Morphology I, p. 1-466). New York: Ithaca.

Scheyer, T. M., Klein, N., & Sander, P. M. (2010). Developmental palaeontology of Reptilia as revealed by histological studies. *Seminars in Cell and Developmental Biology*, 21(4), 462-470.

Schuett, G. W., Reiserer, R. S., & Earley, R. L. (2009). The evolution of bipedal postures in varanoid lizards. *Biological Journal of the Linnean Society*, 97(3), 652-663.

Schulte, J. A., Melville, J., & Larson, A. (2003). Molecular phylogenetic evidence for ancient divergence of lizard taxa on either side of Wallace's Line. *Proceedings of the Royal Society, London B*, 270, 597-603.

Simões TR, Vernygora O, Paparella I, Jimenez-Huidobro P, & Caldwell MW (2017) Mosasauroid phylogeny under multiple phylogenetic methods provides new insights on the evolution of aquatic adaptations in the group. *PLoS One*, 12(5), e0176773. https://doi.org/10.1371/journal.pone.0176773

Smith, K. T. (2009). A new lizard assemblage from the earliest Eocene (Zone Wa0) of the Bighorn Basin, Wyoming, USA: biogeography during the warmest interval of the Cenozoic. *Journal of Systematic Palaeontology*, 7(03), 299-358.

Smith, K. T., Bhullar, B.-A. S., & Holroyd, P. A. (2008). Earliest African record of the *Varanus* stem-clade (Squamata: Varanidae) from the early Oligocene of Egypt. *Journal of Vertebrate Paleontology*, 28(3), 909-913.

Smith, K. T., Habersetzer J. (2021). The anatomy, phylogenetic relationships, and autecology of the carnivorous lizard "*Saniwa*" *feisti* Stritzke, 1983 from the

Eocene of Messel, Germany, in Folie, A., Buffetaut, E., Bardet, N., Houssaye, A., Gheerbrant E. & Laurin, M. (eds), Palaeobiology and Palaeobiogeography of Amphibians and Reptiles: An homage to Jean-Claude Rage. *Comptes Rendus Palevol*, 20(23), 441-506. https://doi.org/10.5852/cr-palevol2021v20a23

Sun, X., & Wang, P. (2005). How old is the Asian monsoon system?—Palaeobotanical records from China. *Palaeogeography, Palaeoclimatology, Palaeoecology*, 222(3-4), 181-222.

Tchobanov, R. 2015. Nahrungsaufnahme bei *Shinisaurus crocodilurus* (Ahl, 1930). Unpublished Masters Thesis, University of Vienna. http://othes.univie.ac.at/37959/1/2015-06-22_0706601.pdf

The Deep Scaly Project, (2011), "*Lanthanotus borneensis*" (On-line), Digital Morphology. Accessed August 7, 2021 at http://digimorph.org/specimens/*Lanthanotus_borneensis*/ATOL/.

Thompson, G. G., & Withers, P. C. (1997). Comparative morphology of western Australian varanid lizards (Squamata: Varanidae). *Journal of Morphology*, 233(2), 127-152.

Thompson, G. G., Clemente, C. J., Withers, P. C., Fry, B. G., & Norman, J. A. (2008). Is body shape of varanid lizards linked with retreat choice. *Australian Journal of Zoology*, 56(5), 351.

Vidal, N., Marin, J., Sassi, J., Battistuzzi, F. U., Donnellan, S., Fitch, A. J. et al. (2012). Molecular evidence for an Asian origin of monitor lizards followed by Tertiary dispersals to Africa and Australasia. *Biology Letters*, 8(5), 853-855.

Villa, A., Abella, J., Alba, D. M., Almécija, S., Bolet, A., Koufos, G. D. et al. (2018). Revision of *Varanus marathonensis* (Squamata, Varanidae) based on historical and new material: morphology, systematics, and paleobiogeography of the European monitor lizards. *PLoS One*, 13(12), e0207719.

Villaseñor-Amador, D., Suárez, N. X., & Alberto Cruz, J. (2021). Bipedalism in Mexican Albian lizard (Squamata) and the locomotion type in other Cretaceous lizards. *Journal of South American Earth Sciences*, 103299.

Wang, Y. (1995). A new primitive chalicothere (Perissodactyla, Mammalia) from the early Eocene of Hubei, China. *Vertebrata PalAsiatica*, 33(2), 138-159 (in Chinese).

Wang, Y., Li, Q., Bai, B., Jin, X., Mao, F., & Meng, J. (2019). Paleogene integrative stratigraphy and timescale of China. *Science China Earth Sciences*, 24.

Werneburg, I., Polachowski, K. M., & Hutchinson, M. N. (2015). Bony skull development in the Argus monitor (Squamata, Varanidae, *Varanus panoptes*) with comments on developmental timing and adult anatomy. *Zoology (Jena)*, 118(4), 255-280.

Zerova, G. A., & Chkhikvadze, V. M. (1986). Neogene varanids of the USSR. *Studies in Herpetology,* Rocek Z. (ed.), *Proceedings of the European Herpetological Meeting*, Prague, 1985, 689-694.

Zhao, Q., Benton, M., Hayashi, S., & Xu, X. (2019). Long bone histology and growth patterns of *Psittacosaurus lujiatunensis* (Dinosauria: Ceratopsia). *Acta Palaeontologica Polonica*, 64, 323-334

Zhu, M., Ding, Z., Wang, X., Chen, Z., Jiang, H., Dong, X. et al. (2010). High-resolution carbon isotope record for the Paleocene-Eocene thermal maximum from the Nanyang Basin, Central China. *Chinese Science Bulletin*, 55(31), 3606-3611.

Acknowledgements
The specimen was collected by Mr. Wei Zhou, Mr. Xun Jin and Mr. Shijie Li, and prepared by Mr. Shuhua Xie, Mr. Long Xiang and Mrs. Yanfang Guo to expose the bones, to detach the skull and the vertebrae from the block, and to prepare the fibula and ribs for histology. We are greatly indebted to these people. We are also grateful to Mr. Wei Gao for photography, Mr. Yemao Hou for scanning, and Ms. Shukang Zhang for preparing the histological sections. We thank Dr. Patrick Campbell for allowing one of us (DLP) to check and measure specimens from the extant *Varanus* collection at the Natural History Museum, London, Dr. Min Wang for discussion, Dr. Jingsong Shi for extant *Varanus* and *Heloderma* disarticulated bones, and Dr. Ryoko Matsumoto, Kanagawa Prefectural Museum of Natural History, for the CT scan of *Lanthanotus* donated to the Evans lab, UCL. We also thank the editor and reviewers for their helpful comments on early versions of the manuscript.

Funding
This work was supported by the National Natural Science Foundation of China (Grant No. 41688103, 42072031, 41702019), the Strategic Priority Research Program (B) of Chinese Academy of Sciences (Grant No. XDB 18000000), Youth Innovation Promotion Association (to DLP), an Anne Sleep Award from the Linnaean Society of London in 2018 to allow DLP to travel to London, and Swiss National Science Foundation (Grant No. 181041) to DV.

Figure captions

Figure 1 Photograph (A) of the holotype specimen IVPP V 22770 of *Archaeovaranus lii* and a close-up of the postcranial skeleton (B). The blue rectangle in (A) indicates the area present in (B); the red rectangle indicates the part present in Figure S4A; the green rectangle indicates the part shown in Figure S4D.
Abbreviations: as, astragalus; ax, axis; ca, calcaneus; caV, caudal vertebra; ceV, cervical vertebra; cor, coracoid; fe, femur; fi, fibula; hu, humerus; L, left; mt, metatarsal; pha, phalanx; postden, postdentary part of mandible; qu, quadrate; R, right; saV, sacral vertebra; sca, scapula; ti, tibia; trV, trunk vertebra; trV-p, posterior trunk vertebra

Figure 2 The cranium of the *Archaeovaranus lii* holotype (IVPP V 22770): A, B, C. 3D renders in dorsal (A), ventral (B) and lateral (C) views; D, E. 3D renders of the braincase in anterior (D) and posterolateral (E) views. D and E are not to scale.
Abbreviations: aip, anterior inferior process of prootic; as.so, ascending process of supraoccipital; a.pro, alar process of prootic; a.sp, alar process of sphenoid; a.vc, anterior opening of vidian canal; bc, braincase; bo, basioccipital; bo.co, basioccipital condyle; bpt, basipterygoid; b.tb, basal tubercle; cr.pro, crista prootica; ecpt, ectopterygoid; ept, epipterygoid; f.6, foramen for abducens nerve; f.7, foramen for facial nerve; f.12, foramen for hypoglossal nerve; f.mg, foramen magnum; fr, frontal; f.o, fenestra ovalis; icf, internal carotid foramen; i.p, incisura prootica; ju, jugal; lac, lacrimal; lrst, lateral opening of recessus scalae tympani; ma, maxilla; na, nasal; ot, otooccipital; pa, parietal; pal, palatine; palp, palpebral; pm, premaxilla; pocc, paroccipital process; pob, postorbital; pof, postfrontal; prf, prefrontal; pro, prootic; psp, parasphenoid; pt, pterygoid; p.vc, posterior opening of vidian canal; qu, quadrate; sm, septomaxilla; sph, sphenoid; sq, squamosal; st, supratemporal; v.f, vagus foramen; vo, vomer

Figure 3 A. Time-scaled phylogeny of Varanidae and its living and fossil relatives. The tree is a simplified version of the strict consensus tree (Figure S23) derived from the analysis based on Villa et al.'s (2018) combined matrix. See supplementary Text S3 for the detailed settings. The subgenera *Empagusia*, *Euprepiosaurus*, *Hapturosaurus*, *Odatria, Soterosaurus*, *Varanus* follow Auliya & Koch (2020) and Brennan et al. (2021). The geographic distributions of the different clades of living *Varanus* refer to Pianka et al. (2004): the Indo-Australian clade is distributed in the yellow and purple regions whereas the Indo-Asian B clade in the purple region and the darker yellow region of Australia; the African and Indo-Asian A clades are in the blue and green regions respectively. The skull of *Varanus prasinus* displays an enclosed bony frontal olfactory canal (transverse section within inset square) and the incomplete bony postorbital bar (blue arrow) whereas the skull of *Archaeovaranus lii* displays the open frontal olfactory canal (transverse section within inset square) and the complete bony postorbital bar (red arrow), conditions also present in other stem varanids such as *Saniwa ensidens* and *Telmasaurus grangeri*, as well as the living *Lanthanotus*. The synapomorphies supporting the nodes, labelled as a, b, c, d, e, are listed in supplementary Text S4. B. Geographical distribution of the fossil varanid relatives, with the colours of the dots representing the temporal distribution of each taxon (corresponding to the colours used on the time chart in A). The green triangles indicate the distribution of the extant *Varanus*.

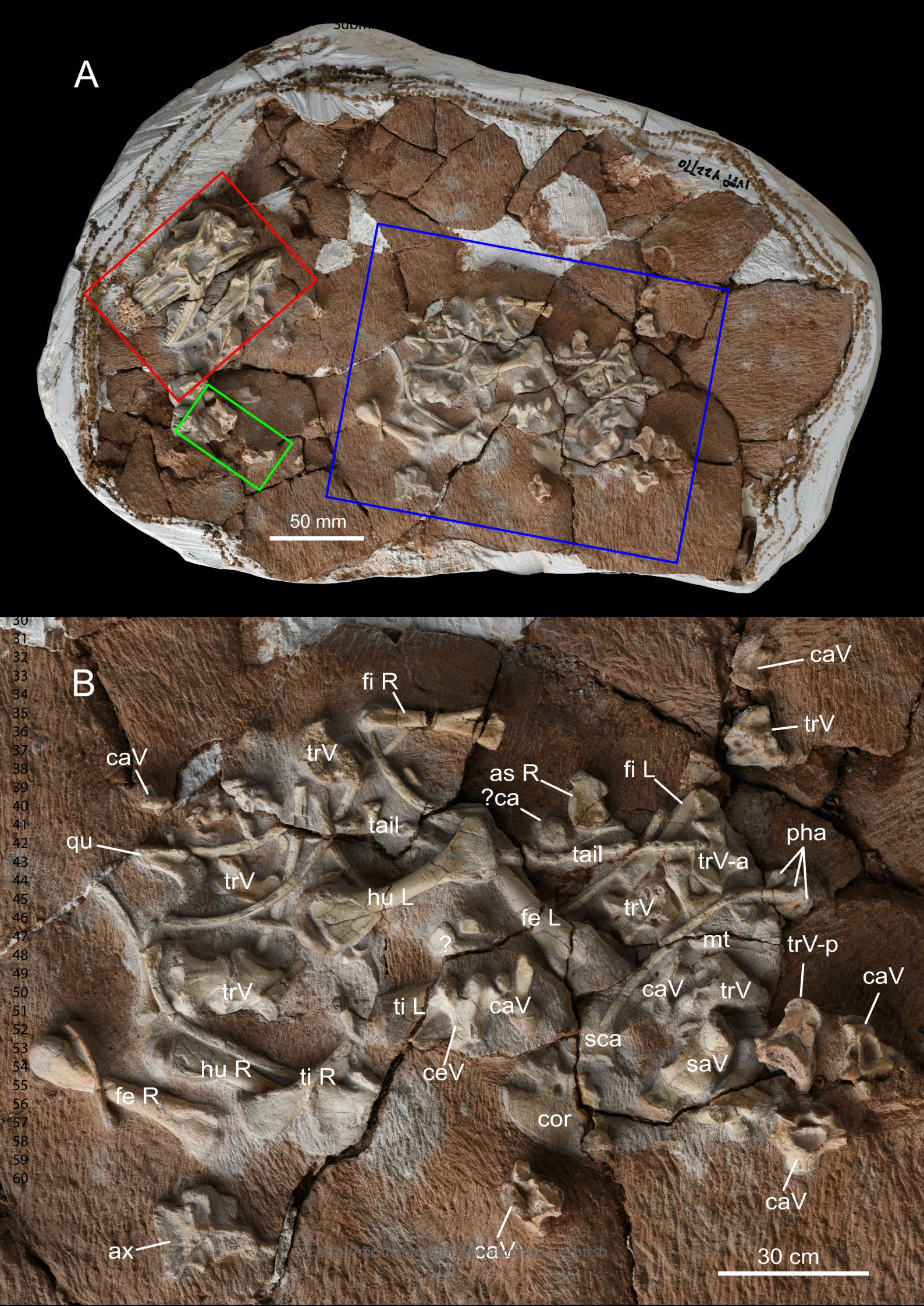
A
50 mm
B
fi R
caV
trV
caV
trV
as R
?ca
fi L
tail
qu
trV
tail
trV-a
pha
hu L
fe L
trV
?
mt
trV-p
caV
trV
caV
ti L
caV
caV
trV
sca
hu R
ti R
ceV
saV
fe R
cor
caV
caV
ax
30 cm

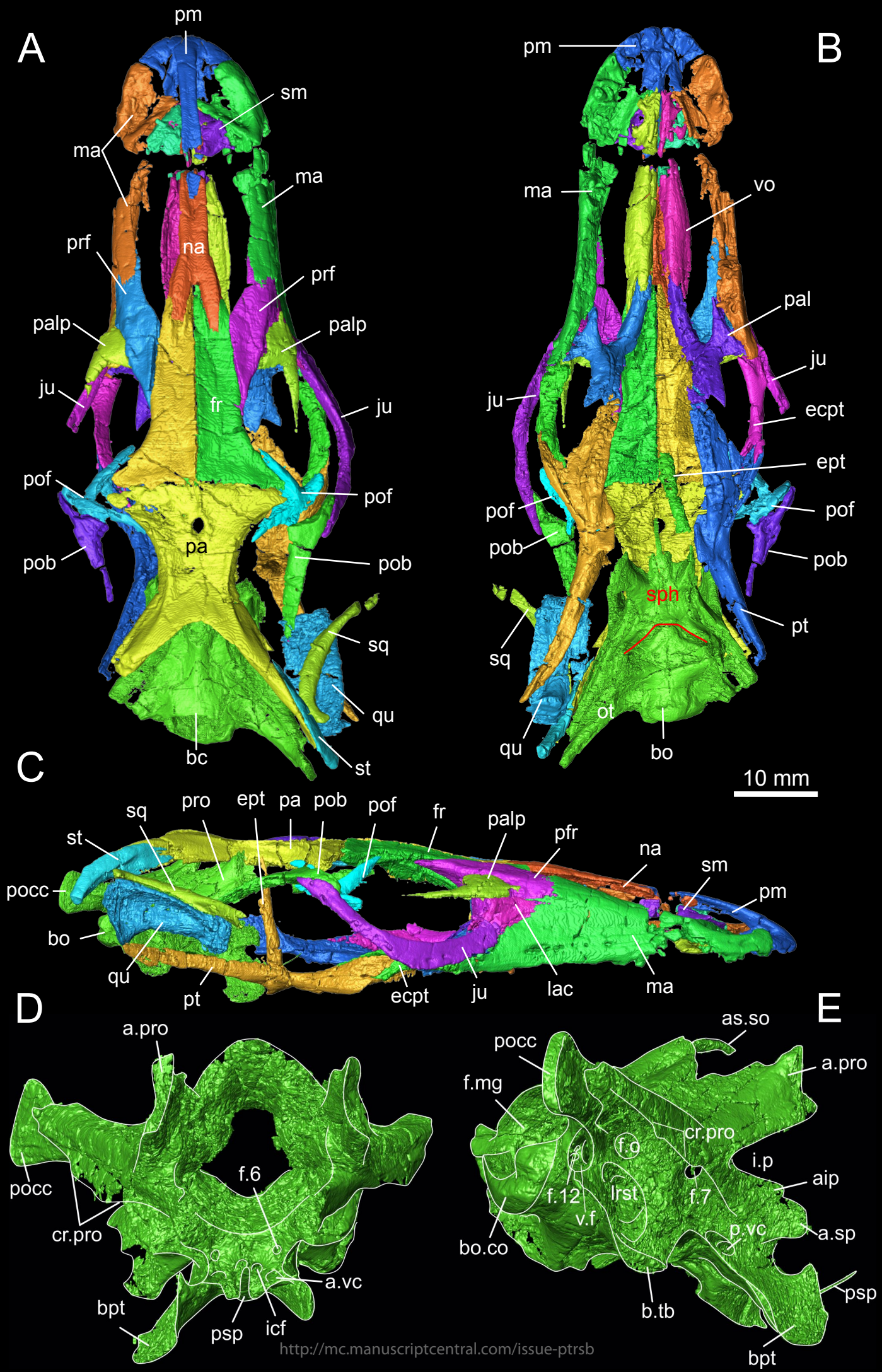
A
pm
sm
ma
ma
prf
na
prf
palp
palp
ju
fr
ju
pof
pof
pa
pob
pob
sq
qu
bc
st
B
pm
ma
vo
pal
ju
ju
ecpt
ept
pof
pof
pob
pob
sph
pt
sq
ot
qu
bo
10 mm
C
sq
pro
ept
pa
pob
pof
fr
palp
pfr
na
sm
pm
st
pocc
bo
qu
pt
ecpt
ju
lac
ma
D
a.pro
pocc
f.6
cr.pro
a.vc
bpt
psp
icf
E
as.so
pocc
a.pro
f.mg
cr.pro
f.9
i.p
aip
f.12
lrst
f.7
v.f
p.vc
a.sp
bo.co
psp
b.tb
bpt
http://mc.manuscriptcentral.com/issue-ptrsb

A

Late Cret. | Paleoc. | Eoc. | Oligoc. | Mioc. | Plioc. | Quat.

Heloderma suspectum
Shinisaurus crocodilurus
Eosaniwa koehni
Paranecrosaurus feisti
Ophisauriscus eucarinatus
Palaeovaranus cayluxi
Lanthanotus borneensis
Cherminotus longifrons
Ovoo gurvel
Telmasaurus grangeri
Aiolosaurus oriens
Saniwides mongoliensis
Paravaranus angustifrons
Proplatynotia longirostrata
Saniwa ensidens
Archaeovaranus lii
Varanus mokrensis
Varanus hooijeri
Varanus cf. *bengalensis*
Varanus rusingensis
Varanus ornatus
Varanus exanthematicus
Varanus albigularis
Varanus niloticus
Varanus griseus
Varanus olivaceus
Hapturosaurus sgen
Euprepiosaurus sgen
Varanus marathonesis
Empagusia sgen
Soterosaurus sgen
Varanus sgen
Odatria sgen

a b c d e

African
Indo-Asian B
Indo-Asian A
Indo-Australian

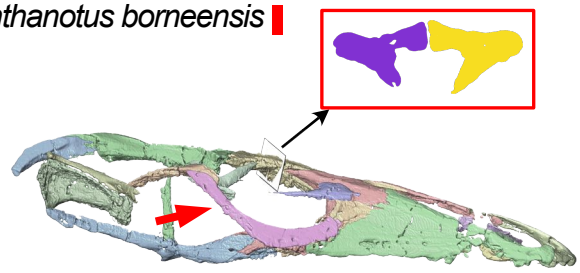

Archaeovaranus lii

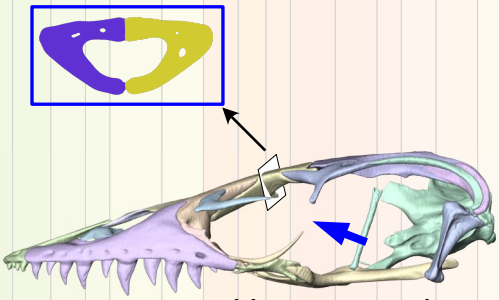

Varanus prasinus

B